HYDROLYSIS PRODUCTS GENERATED BY LIPOPROTEIN LIPASE AND THEIR ASSOCIATION WITH OXIDATIVE STRESS IN THP-1 MACROPHAGES

by © Marzana Monefa, B.Pharm

A thesis submitted to the School of Graduate Studies in partial fulfillment of the

requirements for the degree of

Master of Science

Department of Biochemistry, Faculty of Science

Memorial University of Newfoundland

May 2022

St. John's, Newfoundland and Labrador

Abstract

Lipoprotein lipase (LPL) is an extracellular lipase that hydrolyzes triglycerides (TG) from TG-rich lipoproteins (Lp) within the bloodstream. In the arteries, macrophage LPL expression has been observed to negatively influence atherosclerosis and promote cardiovascular disease. Previously, our laboratory reported that Lp hydrolysis products (HPs) generated by LPL resulted in the upregulated expression of 63 small nucleolar RNAs (snoRNA) within the human macrophage cell. Interestingly, the very low-density lipoprotein (VLDL) HPs by LPL induced the production of reactive oxygen species (ROS), and the cell stress further induced the snoRNA expression in various cell models. The inhibition of NADPH oxidase (NOX) in the cell models diminished snoRNA expression. This project aimed to assess the role of Lp HPs by LPL in oxidative stress using *in vitro* and *in silico* approaches. For *in vitro* studies, human VLDL and chylomicron (CM) HPs generated by LPL were incubated with THP-1 macrophages, with or without a NOX inhibitor (NOXi). The ROS production and lipid peroxidation in the media and cells were analyzed. With an increase in free fatty acid (FFA) concentration from both Lp HPs by LPL, relative to control, there was a decreasing trend in ROS generation for the lowest FFA concentration followed by increasing trend for other FFA concentrations. However, when THP-1 cells were incubated with 0.5 nmol/μL FFA of both Lps HPs by LPL, there was a reduction in ROS with NOXi treatment relative to control. Extracellular ROS was higher with NOXi with 0.5 nmol/μL FFA from VLDL. On the other hand, no change in media malondialdehyde (MDA) with both Lps HPs by LPL was decreased with the addition

of NOXi, while the cellular MDA was decreased with or without NOXi. For *in silico* analyses, available transcriptomic datasets for Lp lipolysis by LPL in two cell lines showed an upregulation of stress-inducing genes and a downregulation of genes associated with cell cycle arrest. Henceforth, my study indicated that Lp HPs by LPL may stimulate foam cell conversion through enhanced NOX-mediated ROS and extracellular MDA levels, which may lead to cellular stress and cell death.

Acknowledgements

First, I would like to thank my supervisor Dr. Robert Brown for his unequivocal support and constant guidance throughout my program. I am very grateful to have had an excellent supervisor who allowed me to grow both academically and professionally despite of adversity. I would also like to thank my supervisory committee members, Dr. Sherri Christian for her advice on the bioinformatics study and Dr. Valerie Booth for her comments on this thesis. I also want to acknowledge my great lab mates over the past couple of years, especially, Kandeepan Karthigesu who assisted me with experimental techniques and provided invaluable suggestions for this study. Furthermore, I would like to pay special thanks to a former graduate student at our lab, Alexandria Tobin, who helped at the beginning of the program by providing training on common experimental techniques used in our lab. Finally, I want to thank my parents and friends, especially my best friend Dr. Inshira Islam, who believed in me and supported me while I finished this degree.

Table of contents

List of tables

List of figures

List of abbreviations

A/A	Antibiotic/antimycotic
ABCA1	ATP-binding cassette transporter A1
Akt	Protein kinase B
apoB	Apolipoprotein B
ARE	Antioxidant response element
ATCC	American Type Culture Collection
BCA	Bicinchonic acid
BSA	Bovine serum albumin
CD36	Cluster of differentiation 36
CM	Chylomicron
CVD	Cardiovascular disease
DEG	Differentially expressed genes
DMEM	Dulbecco's Modified Eagle Medium
DMSO	Dimethyl sulfoxide
DNA	Deoxyribonucleic acid
EC	Endothelial cell
EDTA	Ethylenediaminetetraacetic acid
ER	Endoplasmic reticulum
ERK	Extracellular signal-related kinase

FAF	Fatty acid-free
FBS	Fetal bovine serum
FFA	Free fatty acid
GEO	Gene Expression Omnibus
GPIHBP1	Glycosylphosphatidylinositol-anchored high-density lipoprotein-binding protein 1
GTP	Guanosine-5'-triphosphate
HAEC	Human aortic endothelial cell
HDL	High-density lipoprotein
HEK-293	Human embryonic kidney-293
HP	Hydrolysis product
HSPG	Heparan sulfate proteoglycan
IDL	Intermediate-density lipoprotein
JNK	Jun N-terminal kinase
LDL	Low-density lipoprotein
LDLR	Low-density lipoprotein receptor
Lp	Lipoprotein
LMF1	Lipase maturation factor 1
LPL	Lipoprotein lipase
LRP	LDL receptor-related protein

MAPK	Mitogen-activated protein kinase
M-CSF	Macrophage colony-stimulating factor
MDA	Malondialdehyde
MMP	Matrix metalloproteinase
mRNA	Messenger RNA
mTOR	Mechanistic target of rapamycin
NADPH	Nicotinamide adenine dinucleotide phosphate
NEFA	Non-esterified free fatty acid
NOX	NADPH oxidase
NOXi	NADPH oxidase inhibitor
Nrf2	Nuclear factor-erythroid factor 2
PBS	Phosphate-buffered saline
PI3K	Phosphoinositide 3-kinase
PL	Phospholipid
PMA	Phorbol 12-myristate-13-acetate
PUFA	Polyunsaturated fatty acid
RCT	Reverse cholesterol transport
RNA	Ribonucleic acid

ROS	Reactive oxygen species
RPMI	Roswell Park Memorial Institute
rRNA	Ribosomal ribonucleic acid
SDS-PAGE	Sodium dodecyl sulfide polyacrylamide gel electrophoresis
SMC	Smooth muscle cell
snoRNA	Small nucleolar RNA
SOD	Superoxide dismutase
SR-B1	Scavenger receptor class-B type 1
TAC	Transcriptome analysis console
TBA	Thiobarbituric acid
TBHP	*Tert*-butyl hydroperoxide
TBS	Tris-buffered saline
TG	Triglyceride
TGS	Tris-glycine-sodium dodecyl-sulfate
THL	Tetrahydrolypstatin
TNFα	Tumor necrosis factor α
VLDL	Very low-density lipoprotein
VSMC	Vascular smooth muscle cell

Chapter 1: Introduction

1.1. Atherosclerosis

Even though many advancements have been made in the field of cardiovascular disease (CVD) with respect to diagnosis and treatment, CVD was still the second leading cause of death in Canada from 2015 to 2019. In 2019, it has been estimated that approximately 17.9 million people globally died due to CVDs alone. The mortality rate due to CVDs accounts for 32% of all global deaths, making it the leading cause of global mortality. From 1990 to 2019, the prevalent cases of total CVD have roughly doubled, along with the steady increase of CVD deaths [1]. Pathologically, atherosclerosis is the root cause of most CVD occurrence, stroke, and peripheral arterial diseases, hence several researchers study the pathophysiology of it [1]. Atherosclerosis plays a key role in vascular diseases and is characterized by a thickening of the intima by an accumulation of inflammatory cells, fibrous elements, and lipids that form plaque deposition at endothelial cell (EC) injury and constriction of the arteries [2]. During atherogenesis, studies on pathology have shown cellular and molecular interactions in the arteries with a defined series of changes in the vessel, as shown in Figure 1.1, where the macrophage plays the most crucial role [2, 3]. The injured endothelium mediates inflammation by recruiting monocytes where monocytes differentiate into macrophages and accumulate oxidatively modified low-density lipoprotein (LDL), following the conversion of macrophage into foam cells [4]. Thus, extensive research has been focused in understanding the complex molecular and cellular processes with the involvement of foam cells in understanding atherosclerosis processes.

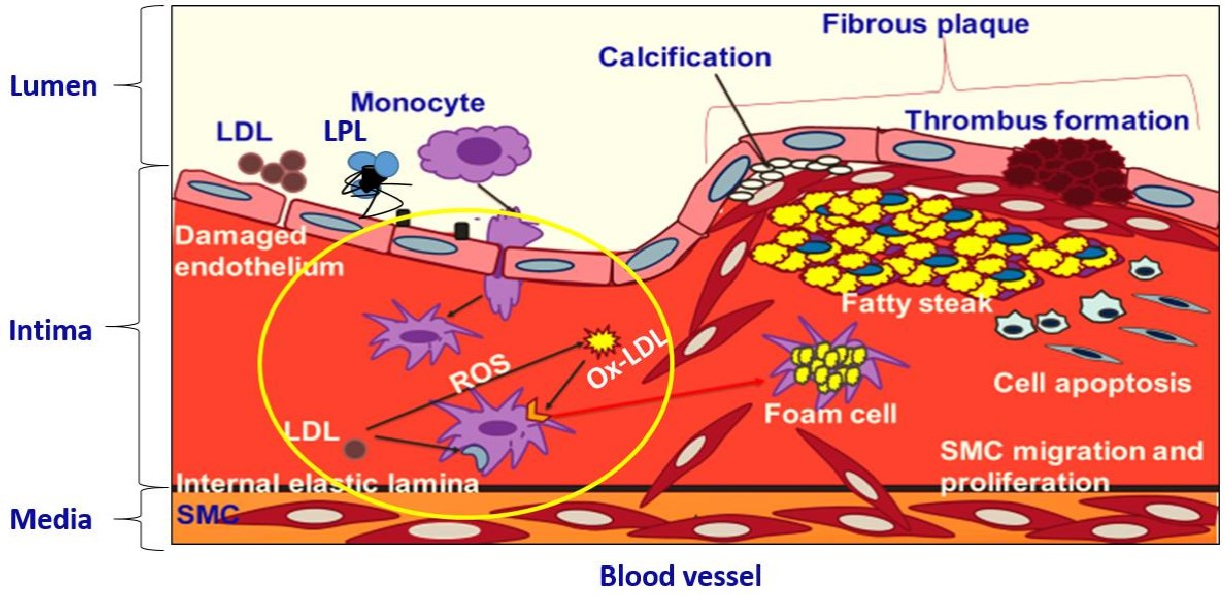

Figure 1.1: The pathogenesis of atherosclerosis

Triglyceride-rich lipoproteins (Lp) are hydrolyzed by lipoprotein lipase that is bound to the EC. LDL enters the intima through sites of damaged EC. In the intima, initial lesion formation begins, and it undergoes alterations, such as oxidation by reactive oxygen species (ROS), which recruits monocytes. The monocytes convert to macrophages, and these macrophages uptake oxidatively modified LDL to form foam cells. Smooth muscle cells (SMC) then start to proliferate and migrate toward the intima where they contribute to forming foam cells. The lipid laden foam cells form fibrous plaques through calcification, and trigger a complex inflammatory response causing rupture of plaque and leading to thrombosis. Figure 1.1 was drawn using Microsoft PowerPoint.

1.1.1. Stages of atherosclerosis

Lesion initiation occurs during the first stage of atherosclerosis. The endothelium of blood vessels acts as a barrier between blood and tissue. Lesion formation preferentially takes place where the blood flow is disturbed, in regions of arterial branching or curvature, and it results in increased permeability to macromolecules such as LDL [5]. The increase in permeability is followed by a build-up of LDL in the sub-endothelial matrix (which is greater when levels of circulating LDL in plasma are higher), causing LDL to be passively transported through EC junctions and retained in the vessel wall for lesion formation. This retention involves interactions between the LDL constituent apolipoprotein B (apoB) and matrix proteoglycans inthe intima [6]. Hence, the initiation of lesion generation comprises of LDL entering and retention in the intima to promote atherosclerosis.

The LDL can be subjected to oxidation, proteolysis, lipolysis and aggregation in the intima, and these modified LDL are taken up by macrophages to convert into foam cells [7]. This modification leads to inflammation and foam cell formation. The vascular cells producing oxidative waste cause the oxidation of lipids, resulting in the early lesion formation. Due to lipid oxidation, pro-inflammatory “minimally oxidized” LDL, an initial product of progressive LDL oxidation, is formed at the beginning of lesion formation, which possesses pro-inflammatory activity but does not bind to the scavenger receptors of macrophages for its uptake [4].

In the next stage when inflammatory reactions start, the accumulation of minimally oxidized LDL species causes enhanced expression of pro-inflammatory molecules, including vascular celladhesion molecules-1, P, and E- selectins, cell adhesion molecules and growth factors like macrophage colony-stimulating factor (M-CSF) in the intima. These adhesion molecules and chemotactic factors have complementary carbohydrate ligands which are present in monocytes, like PSGL-1, to EC selectins, [4, 8, and 9]. Thus, recruited monocytes are involved in forming

lesions.

Once the monocytes are inside the intimal layer, M-CSFstimulates the proliferation and differentiation of monocytes into macrophages, and M-CSF contributes to changes in the macrophage functions, including increased scavenger receptor expression. For the differentiated macrophages to uptake LDL particles rapidly, LDL must be highly oxidized [10]. This alteration of minimally oxidized to highly oxidized LDL (ox-LDL) particles seemingly involves reactive oxygen species (ROS) which are thought to be produced by ECs, macrophages, and enzymes in human atherosclerotic lesions [4]. Therefore, M-CSF is crucial for growth and differentiation of monocytes to macrophages, and for macrophages to take up modified LDL.

The internalization of ox-LDL in the macrophages takes place due to a number of receptors that identify a wide range of ligands. The important 'scavenger' receptors include scavenger receptor-A and cluster of differentiation 36 (CD36) [11, 12]; their expression is controlled by the cytokines tumor necrosis factor-α (TNFα) and interferon-γ, and the transcription factor peroxisome proliferator activated receptor-γ [13]. These receptors assist in accelerating the uptake of modified LDL particles by macrophages, leading to foam cell formation. The presence of a fatty streak in the intima of artery demonstrates a hallmark of early atherosclerosis lesion.

Cytokines and growth factors secreted by macrophages and T-cells stimulate the proliferationand migration of smooth muscle cells (SMC) and the production of extracellular matrix proteins [4, 14]. Over time, death of foam cells takes place, and their lipid-filled content contributes to thenecrotic core of the lesion. In the intima, the accumulation of migrating SMCs occurs in some fatty streaks. Additionally, the SMCs secrete fibrous elements which produce occlusive fibrous plaquesthat tend to increase in size with time. Fibrous plaques are identified by a developing mass of extracellular lipid, chiefly cholesterol, cholesteryl esters, and by the buildup of SMCs andextracellular matrix derived from them [4]. Henceforth, SMC, foam cells and the

extracellular matrix are involved in the plaque formation.

The content and vulnerability of the fibrous plaques are important in thrombus development. Thin fibrous caps and an increased number of inflammatory cells are characteristic of vulnerable plaques. Fibrous cap retention depends on maintaining a balance between the production of matrix and matrix degradation, and inflammatory cell products presumably mediate both processes. The lesion edges are more prone to ruptures, and they are composed of foam cells. Moreover, neovascularization and calcification, which are known advanced lesion features, play roles in stabilizing atherosclerotic lesions [4]. In neovascularization, there is an influx of inflammatory cells from the growing small vessels, which further reinforces the atherosclerotic lesions. The ox-LDLhave been reported to produce tissue factor, the presence of which affects the thrombogenicity of the lesion core [15]. Because of narrow fibrous cap and entrance of inflammatory molecules, the vulnerable plaque ruptures and generates a thrombus.

1.2. Lipoprotein metabolism and lipases

1.2.1. Lipids

There are several classes of lipids that associate with proteins in the cell membrane that provide important structural functions, can act as signaling molecules, and deliver energy to cells via oxidation. The energy source is obtained from the lipid intake via diet or lipids formed endogenously in the body. Lipids can act as energy storages in the body, can be easily utilized by the cells whenever required, and allow for survival without taking in any food for up to several weeks. In diet, cholesterol intake is not essential as adequate amounts are synthesized in the body. Even though cholesterol is important as a structural component of cells, the pathological accumulation of cholesterol in the artery walls leads to atherosclerosis and CVD.

1.2.2. Lipoproteins

As lipids (including TGs and cholesterols) are partially soluble in water, they require associated proteins for being transported in the circulation. Lps assist in absorption as wellas transportation of dietary and endogenous lipids from the small intestine and liver to the peripheral tissues, and assist in reverse cholesterol transport (RCT) [16,17]. Therefore, Lps aid as a delivery system of lipids to help in performing their functions in the body.

1.2.3. Structure of lipoproteins

The structure of Lps is complex; they consist of a central hydrophobic core enriched with non- polar lipids, cholesteryl esters and TGs. The central core is enclosed by a hydrophilic membranecomprised of free cholesterol, apolipoproteins and phospholipids (PLs) (Figure 1.2) [18]. PlasmaLps are classified based on their size, apolipoprotein content, and lipid content (Table 1). They can be divided into six classes: high-density lipoproteins (HDL), chylomicrons (CM), CM remnants, very low-density lipoprotein (VLDL), intermediate-density lipoprotein (IDL), and LDL. Among these Lp classes, LDL, IDL, VLDL, and CM remnants are pro-atherogenic, whereas HDL is believed to have an anti-atherogenic role. An apolipoprotein is the protein that incorporates with lipid to form a Lp. The composition of the lipid and apolipoprotein plays a key role in the structural formation of Lps. The structure of apolipoproteins is unique and modular, which accounts for their multiple functions. ApoA-I, apoB100, and apoB48 function in assembling and secretion of Lps; apoB, apoE, apoA-I, and apoA-II help in maintaining the structural integrity of Lps. Also, apoA-I, apoA-V, apoC-I, apoC-II, and apoC-III act as coactivators or inhibitors of enzymes [19]. Furthermore, they regulate the cellular uptake of the entire particle or selective uptake of a lipid component of Lps by acting as ligands that bind to the membrane Lp receptors. For instance, apoB100 and apoE bind to the LDL receptor (LDLR) [20], whereas apoE binds to the LDL receptor-related protein (LRP) [21], and apoA binds to scavenger

receptor BI [22]. Hence, the different size, structure, apolipoprotein, and content accounts for various Lps to perform their function.

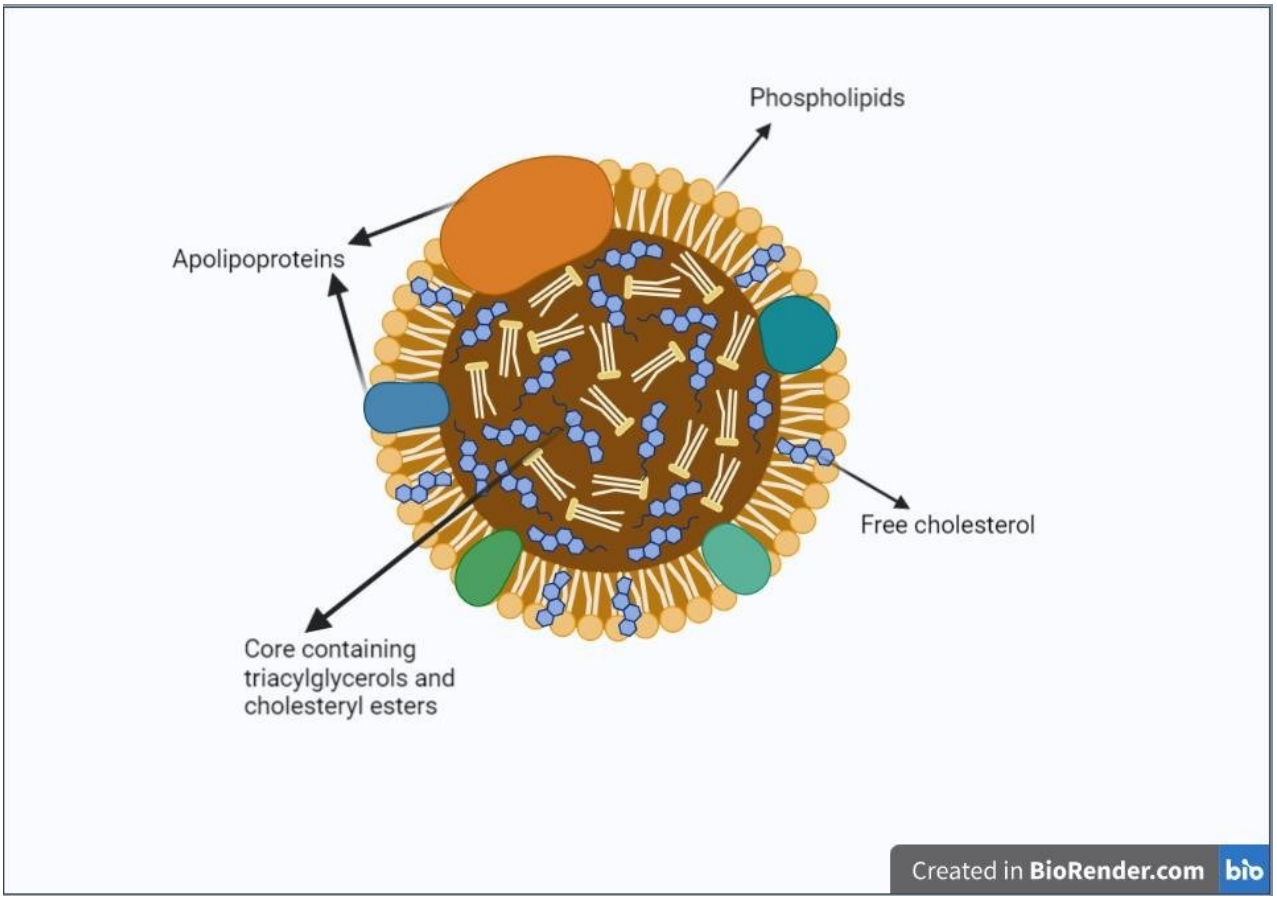

Figure 1.2: Lipoprotein structure

The structural formation of a Lp is complex, consisting of a central hydrophobic core enriched with non-polar lipids, cholesteryl esters and TGs, and enclosed by a hydrophilic membrane comprising of free cholesterol, apolipoproteins and PLs. Figure 1.2 was drawn using BioRender.

Table 1: Lp classification [18]

The lipoproteins are classified into six groups based on their density, the lipid it transports and main apolipoproteins.

Lipoprotein	Size (nm)	Density (g/ml)	Main Lipid	Main Apolipoprotein
HDL	5- 12	1.063-1.210	Cholesterol, Phospholipids	ApoA-I, ApoA-II, ApoC, ApoE
LDL	18- 25	1.019-1.063	Cholesterol	ApoB-100
IDL	25-35	1.006-1.019	Triglycerides, Cholesterol	ApoB-100, ApoE, ApoC
VLDL	30-80	0.930-1.006	Triglycerides	ApoB-100, ApoE, ApoC
CM Remnants	30-80	0.930-1.006	Triglycerides, Cholesterol	ApoB-48, ApoE
CM (CM)	75-1200	<0.930	Triglycerides	ApoB-48, ApoC, ApoE, ApoA-I,A-II,A-IV

1.2.4. Lipoprotein metabolism

In the intestine, dietary lipids are incorporated into CMs. CMs are large Lps composed of high amounts of TG, are synthesized by the small intestine, and carry the dietary TG to peripheral tissues and cholesterol to the liver. The main structural protein of CMs is apoB48.

There is variation in the size of CMs with the amount of dietary fat intake. For instance, larger CM particles will be formed with a high fat diet. The dietary TG is transported via CMs and is then subjected to hydrolysis by LPL in muscle and adipose tissue to liberate free fatty acids (FFA). The released FFA are then utilized by the cells for energy. Thus, the removal of TG fromCMs results in forming CM remnants. In comparison to CMs, CM remnants are enriched in cholesterol and are pro-atherogenic [18]. The rapid hepatic clearance of CM remnants occurs when they reach a smaller size that allows them to pass from the endothelial space to

the perisinusoidal space. Here, they can be directly removed by apoE binding to the LDLR, or/and additional free apoE in the perisinusoidal space can remove remnant particles via LRP. Moreover, the CM remnant may be sequestered in the perisinusoidal space by binding to heparan sulfate proteoglycans (HSPG) via apoE and/or by binding to hepatic lipase (HL) using apoB [23]. Hence, CM are formed in the intestine and to carry dietary lipids, and they are metabolized into CM remnants upon hydrolysis of TG to liberate FFA for cells to utilize energy.

VLDL is synthesized by the liver and it contains one apoB100 molecule. The size of the VLDL depends on the content of TG produced by the liver. Nonetheless, VLDL particles are smaller in size than CMs. In muscle and adipose tissue, VLDL enriched with endogenous TGare metabolized with the aid of LPL anchored to the capillary endothelium, which liberates FFAsand forms IDL.

IDL becomes smaller in size and denser in the circulation through the metabolism of lipids by HL, further enriching the cholesterol content and converting the Lp into LDL. LDL's prime apolipoprotein is B100 and each LDL carries one apoB100 molecule [24, 25]. The uptake of LDL in several peripheral cell types occurs through LDLR. Following uptake of LDL, the cells use the cholesterol content for various functions, including cellular membrane synthesis, lipid raft formation, as precursor of steroid hormones and, in neurodevelopment. The excess LDL in the bloodstream is removed via hepatic clearance, where LDL binds to LDLRs associated with coated pits at the cell surface of the hepatocytes. The complexes formed are internalized through clathrin-coated vesicles to endosomes, where they detach. Following internalization, the LDL particles move into lysosomes and are subjected to degradation, while the LDLRs are recycled to the cell surface [26]. LDL particles have a varied range of sizes and densities in circulation. Smaller and denser LDL particles have been linked to hypertriglyceridemia and type-2 diabetes. The smaller and denser LDL particles are more pro- atherogenic than larger LDL particles for three main reasons. Firstly, small, and dense LDL has decreased affinity toward LDLR, causing them to be retained in the circulation for a longer time. Secondly, the small size allows easier entry to the arterial wall where they bind to intra-arterial proteoglycans and remain trapped in the arterial wall. Finally, it has been reported that small, dense LDL particles are more prone to oxidation, which could lead to enhanced uptake by macrophages [18]. Hence, excess LDL particles contribute to atherosclerosis progression.

Nascent (or pre-β) HDL, the precursor to mature HDL, can be synthesized from apoA-I in various cells but is mainly synthesized by the liver and intestines, which initiates RCT. In this transport, excess cholesterol is carried from peripheral tissues to the liver, and thus HDL is considered anti-atherogenic. HDLs are enriched with cholesterol and PL; their core structural

protein is apoA-I and multiple apoA-1 molecules can be present. Nascent HDL synthesis takes place when apoA-I takes up cholesterol and PL via the adenosine triphosphate-binding cassette transporter, sub-family A, member 1 (ABCA1) [27- 29]. Additionally, more cholesterol can be taken up by the nascent HDL to convert to mature HDL through passive diffusion via adenosine triphosphate-binding cassette subfamily G member 1 and scavenger receptor type-BI (SR-BI). There are two fates of this cholesterol-rich HDL: either the cholesterol is given away to LDL or VLDL in exchange for TG by the cholesteryl ester transfer protein, or the cholesterol is removed from the HDL by hepatic SR-B1. The process of cholesterol efflux from macrophages to HDL has an important protection role against atherosclerosis development [20]. Therefore, HDL plays an athero-protective role in the body.

1.2.5. Lipoprotein lipase

Lp acylglycerides and PLs can be metabolized by the enzymes within the *sn-1* lipase family, by hydrolyzing the ester bonds at the *sn*-1 or *sn*-3 of TG, or the *sn*-1 position of PL, to liberate fatty acids [30]. These lipases include LPL, HL and endothelial lipase. Even though these lipases possess catalytic activity, they have non-catalytic activity, where they function as a molecular bridge, bringing plasma Lp very near to cell surface receptors to facilitate Lp uptake into cells [31]. Therefore, LPL possesses both catalytic and non- catalytic role in Lp hydrolysis.

LPL is an extracellular lipase, incorporated specifically to hydrolyze TG at the *sn*-1 and *sn*-3positions as shown in Figure 1.3 [32, 33]. LPL hydrolyzes the TGs transported in CMs and VLDL to release fatty acids for the cells to utilize, as shown in Figure 1.4. The catabolized TGs lead to conversion of CMs and VLDL into CM remnants and IDL, respectively. For LPL activity, apoC-II acts as a cofactor and activator, whereas apoA-V is an activator of proteoglycan-bound LPL [34]. Contrarily, Apo C-III and Apo A-II inhibit the LPL activity [35].

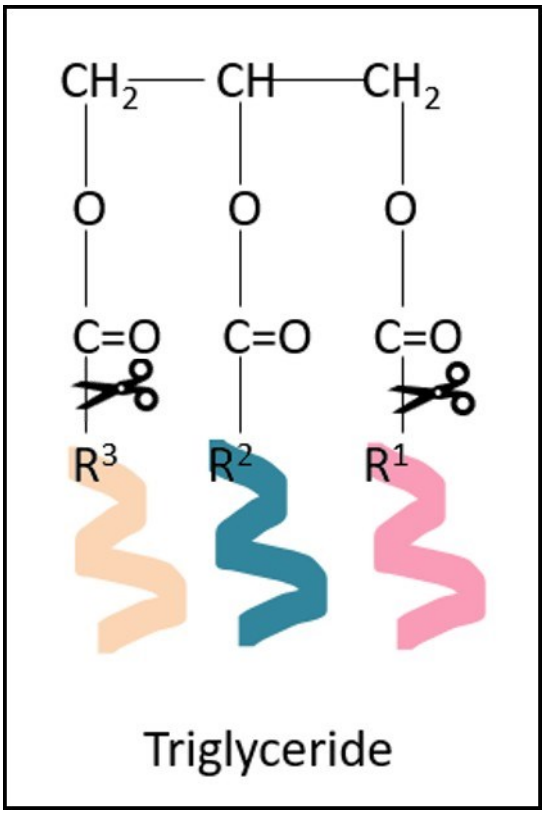

Figure 1.3: The *sn*-1 and *sn*-3 cleavage point of a general triglyceride.

LPL acts at the *sn*-1 and *sn*-3 positions, as shown (scissors), to remove fatty acyl chains, as shown (R^1,R^2,R^3 with pink, blue and beige color, respectively) from TG. Figure 1.3 was drawn using Microsoft PowerPoint.

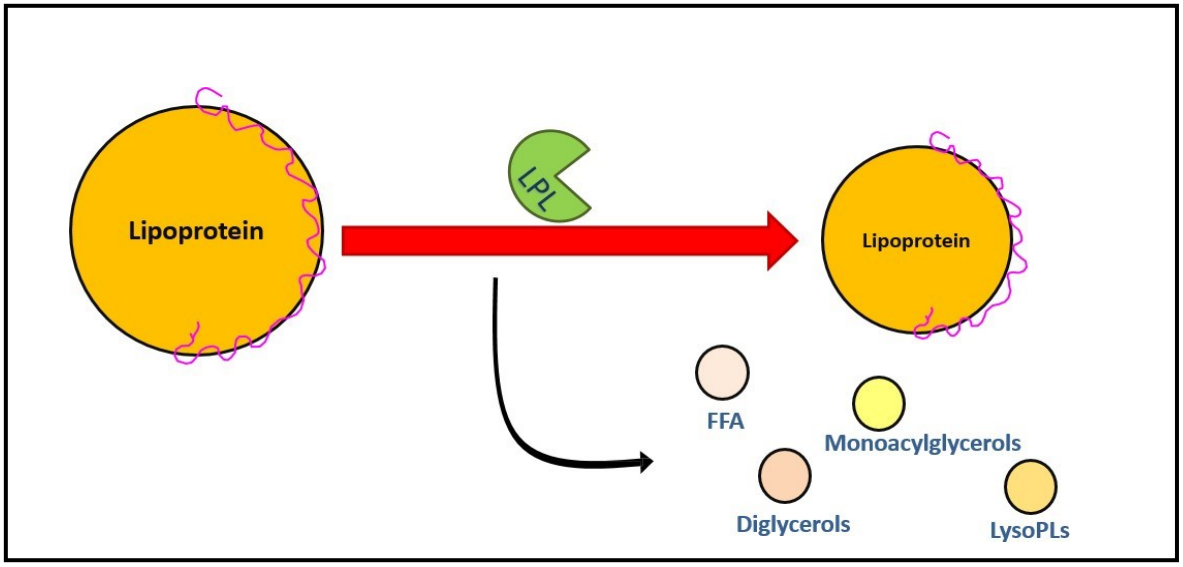

Figure 1.4: LPL hydrolyzes TG-rich Lps.

LPL can generate FFA, di- and monoacylglycerols, and lysoPLs for use by the surrounding cells.

Figure 1.4 was drawn using Microsoft PowerPoint.

Thus, Lp apolipoproteins plays important role in regulating the LPL activity.

LPL has been reported to be expressed in muscle, heart, and adipose tissue and is then secreted by exocytosis. Following secretion, LPL associates with the cell surface protein, glycosyl phosphatidyl inositol-anchored high-density lipoprotein binding protein (GPIHBP1) [36], and with the cell surface through HSPG [37,38]. LPL is abundant in several tissues, including, lungs, heart, spleen, skeletal muscle adipose, mammary glands, monocytes, and macrophages [39–41]. Thus, LPL is expressed in various tissues where it gets secreted to the capillary lumen surface by associating with the GPIHBP1 proteins.

1.2.6. LPL synthesis and processing

LPL is synthesized by the parenchymal cells, where LPL gets transported to the ECs surface. Additionally, LPL is synthesized within fat cells and then is transported to the endothelial stroma of adipose tissue for lipid metabolism. The LPL gene is located at chromosome 8p22, which produces the LPL protein with 475 amino acids. The mature LPL with 448 amino acids is formed by cleaving a 27 amino acid signal peptide [42]. In the rough endoplasmic reticulum (ER), *LPL* mRNA (messenger ribonucleic acid) is translated toLPL and then transported through the *cis*- and *trans*- Golgi network, where LPL is highly glycosylated. The glycosylation accounts for 8-12 % of LPL mass, converting it from 51 kDa of subunit mass to 55 kDa. The final conformation of functional LPL has been probed using ultracentrifugation and was found to be homodimer [43]. Although, it has recently been suggested that LPL bound to an accessory protein may function as a monomer [44]. Hence, LPL is produced in the parenchymal cells, where it is subjected to glycosylation and the functional LPL gets delivered to EC surface.

LPL homodimers are organized in a head-to-tail configuration, where an N-terminal β-hydrolase domain contains six alpha-helices and ten β-strands, concealing the catalytic triad: S159, D183, and H268. The C-terminal region comprises of a C-terminal flattened β-barrel domain with twelve β-stands connected with a hinge to the N-terminal region [44].

For LPL to gain its final tertiary structure and for the dimerization to form the homodimers, they need to interact with lipase maturation factor 1 (LMF1), a transmembrane chaperone positioned in the ER [45]. The partially assembled LPL monomers bind to LMF1 to convert to the correct tertiary structure of functional LPL homodimers and are secreted to the interstitial space. If there is a misfolding of LPL, it is subjected to degradation in the ER. Misfolded LPL buildup in the ER is usually a consequence of LMF1 expression-related disorders [46]. Upon secretion of functional LPL from the parenchymal cells to the interstitial space, it binds to HSPG and gets translocated to GPIHBP1 attached to ECs, as LPL has higher binding affinity towards GPIHBP1 [47, 48]. Knockout studies of GPIHBP1 demonstrated that LPL remains associated to HSPG in the interstitial space, and this leads to lowering of LPL activity in blood. The loss of GPIHBP1 expression results in LPL to become trapped in the interstitial space, causing a significant reduction of LPL activity. The crystal structure of the LPL-GPIHBP1 complex showed that the LPL C-terminal domain and GPIHBP1 associate with each other at 1:1 ratio. Moreover, LPL affinity was proven to be higher for GPIHBP1 than HSPG, using *in vivo* and *in vitro* studies [49]. Hence, the LPL-GPIHBP1 complex in the endothelium surface, facing the lumen of the capillaries, hydrolyzes Lps to ensure they reach the tissues that require them (Figure 1.5).

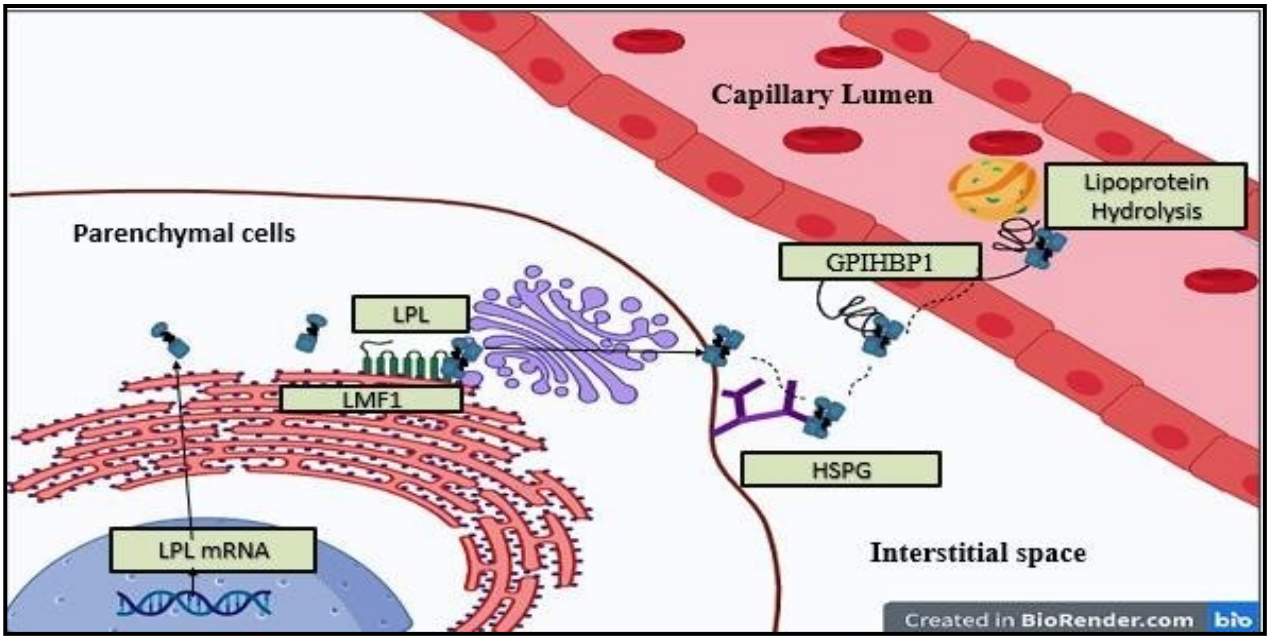

Figure 1.5: LPL secretion from parenchymal cells to the vascular endothelial surface.

LPL mRNA produced in tissue parenchymal cells are translated into LPL monomers in the ER. LMF1 in the ER binds to the LPL monomers to aid in assembling and dimerization mature LPL. The mature LPL is glycosylated in the ER and after moving through the Golgi apparatus, it is secreted into the interstitial space where it binds to HSPG nearby. From HSPG, the mature LPL is shuttled to endothelial-bound GPIHBP1 to hydrolyze circulating Lps. Figure 1.5 was drawn using Biorender and Microsoft PowerPoint.

1.2.7. Macrophage LPL in atherosclerosis

Macrophages expressing LPL have been linked to atherogenesis [51]. For instance, Takahashi *et al.* [52] showed that macrophages collected from macrophage-specific LPL knockout and apoE double knockout mice fed a Western diet had less build-up of cholesteryl esters and TGs, compared to apoE double knockout mice (control). This study suggested that LPL located in the arterial wall might be derived from macrophages, having a pro-atherogenic effect. Moreover, Wilson *et al.* [52] reported that the increased expression of human LPL in macrophages of the male apoE-null mice which were fed a Western diet for eight weeks demonstrated increased atherosclerotic development in comparison to the control. The hydrolysis products (HPs) liberated by LPL from Lps may contribute to atherosclerosis development. The FFA that were liberated from VLDL by LPL have been reported to enhance increased lipid droplet accumulation in human THP-1 macrophages [53]. Furthermore, when LDL and ox-LDL are captured by the macrophages expressing LPL in the site of atherosclerosis, it suggests LPL helps in converting macrophages to foam cells. These foam cells play a central role in the build-up of plaque and contribute to atherosclerosis [54].

1.3. Oxidative stress in atherosclerosis

One of the most identified characteristics of the pathogenesis of atherosclerosis is oxidative stress, which is observed along with the initiation of pro-inflammatory signaling pathways and cytokine expression. Several studies indicated that the overproduction of ROS is integral to the development of CVD [53, 54]. ROS are formed when atmospheric or cellular oxygen gets partially reduced or excited; this includes superoxide ($O2^{\bullet-}$), hydrogen peroxide ($H2O2$), hydroxyl radicals ($HO^{\bullet}$) and singlet oxygen ($^{1}O2$) [55]. It is essential to maintain a basal level of ROS, as they are physiologically important to cells because they play roles in cellular

processes, signaling and viability.

The reduction of molecular oxygen gives rise to the generation of superoxide. This, superoxide has two fates: it can be converted to diatomic oxygen or, with the help of the mitochondrial enzyme superoxide dismutase (SOD), can form hydrogen peroxide [56]. By the Fenton reaction, hydroxyl radicals are generated from hydrogen peroxide, which itself is moderately unreactive. The hydroxyl radicals possess damaging activity towards cellular structures and molecules. The following net reaction depicts how a molecule of superoxide associates with a molecule of hydrogen peroxide to generate reactive and harmful hydroxyl radicals: $\bullet O_2^- + H_2O_2 \rightarrow \bullet OH + OH^- + O_2$ [57]. Moreover, the formation of the damaging hydroxyl radicals can result from hypochlorous acid reactions, which are produced by the enzyme, myeloperoxidase [58]. In the cell, ROS are generated via many enzymatic pathways, where most enzymatic pathways initiate with superoxide production and results in production of more reactive species. Even though enzymes like nicotinamide adenine dinucleotide phosphate (NADPH) oxidases (NOX) deliberately produce superoxide, ROS can be produced as by-product of metabolism.

These chemically reactive oxygen radicals vary in range of reactivity and show their effect at molecular levels. Despite having beneficial roles in cells, increased ROS causes oxidative stress and plays a significant role in the development of CVDs. Oxidative stress is critical in the formation of atherosclerotic lesions. In atherosclerosis, migration of monocytes, T-lymphocytes and mast cells in the vascular walls account for activation of inflammatory processes and cytokine release, resulting in overproduction of ROS. For example, a study showed mitochondrial ROS was increased proportionally to the level of the cytokine, TNFα [59]. Furthermore, other cytokines, including interferon-γ and interleukin-1, displayed enhanced NOX-mediated ROS

formation [60]. Moreover, increased ROS has been shown to elevate SR expression on vascular SMC, which improves the ability of macrophages to uptake and accumulate lipids to transform into foam cells. Also, ROS stimulates the release of matrix metalloproteinases (MMPs), which aid in plaque disruption and cause thrombosis. It was observed that vascular SMC displaying cyclic strain-induced MMP-2 expression was NOX activation dependent [61]. Hence, ROS at a basal level plays an advantageous role in the body, but enhanced ROS stimulates oxidative stress promoting atherosclerosis.

1.4. The NADPH oxidase and its isoforms

The NADPH oxidases of the NOX family were originally identified in the membranes of phagocytic macrophage cells. As frontliners in innate immunity, macrophages utilize NOX-mediated superoxide, which acts as a powerful primary microbicidal agent, to kill invading pathogens. These enzymes are responsible in catalyzing the conversion of molecular oxygen to superoxide, a ROS, where the NADPH component acts as the electron donor. Moreover, the homologs of NADPH oxidase were later identified in non-phagocytic cells like SMC, fibroblasts, and EC.

To date, seven members of NOX have been identified which includes, NOX1-5 and two large NOX5-like dual oxidases (DUOX), DUOX1 and 2. Among these, NOX2 was the first recognized and most widely investigated member of the NOX family. Notable levels of NOX1, NOX2, NOX4, and NOX5 have been shown to be expressed in the vascular SMCs, endothelium, perivascular adipocytes, and fibroblasts [62]. Hence, NOX expression is abundant in the cells involved in atherosclerosis.

1.4.1. NADPH oxidase structure

All seven members of the NOX family are transmembrane protein complexes consisting of six hetero subunits. In the resting state, four of the enzyme subunits are maintained in the cytosol and have two integral membrane proteins in the enzyme complex. The presence of any stimulus regulates assembly and translocation of the subunits to the membrane, which interact and gain the ability to generate superoxide anions by reducing oxygen. The enzymes have a highly conserved cytosolic C-termini containing a NADPH-binding region following a FAD-binding site. The two transmembrane subunits are p22phox and gp91phox; this heterodimer forms the catalytic core of the enzyme flavocytochrome b558. The catalytic core is controlled by interactions with the cytosolic multidomain subunits: p67phox, p40phox and p47phox, alongsidethe small guanosine-5'-triphosphatase (GTPase) Rac belongs to the Rho family of small GTPases as show in Figure 1.6 [63]. Thus, the NOX enzyme complex consists of cytosolic and transmembrane components, that catalyzes the generation of superoxide from molecular oxygen.

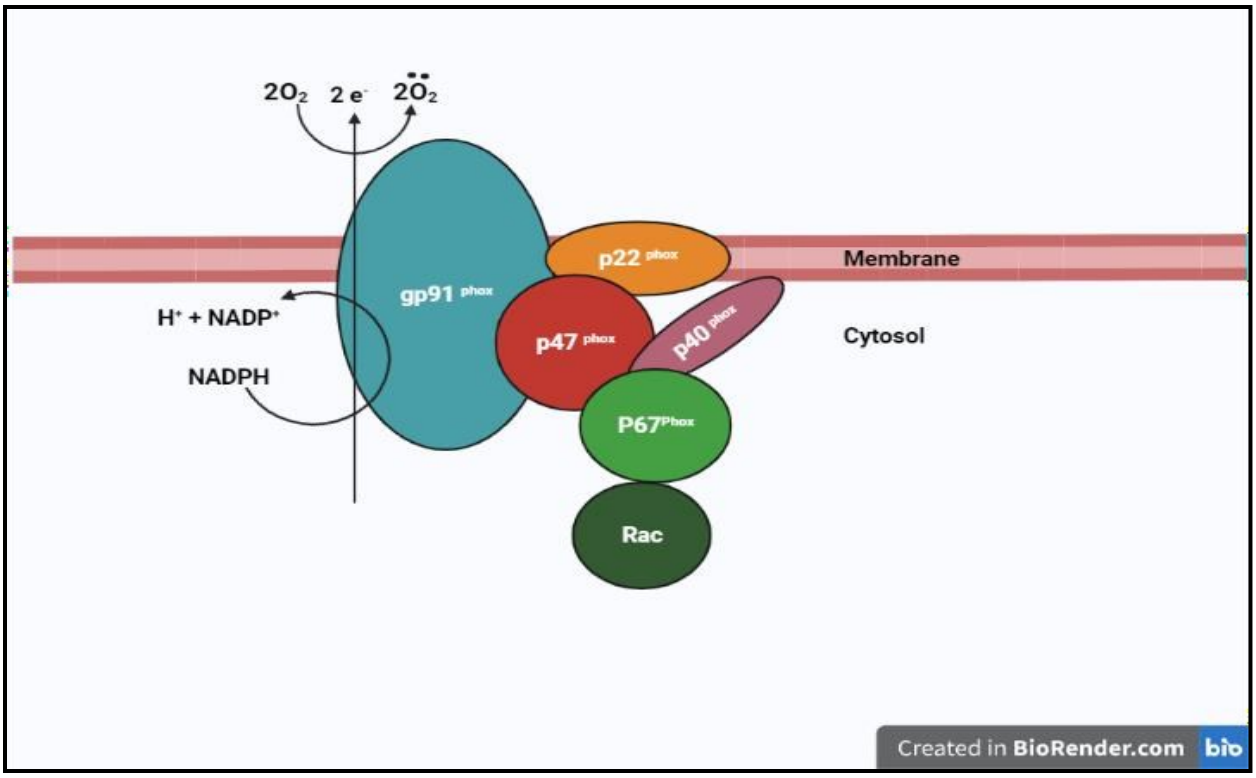

Figure 1.6: The structure of NOX in the plasma membrane

NOX comprises of many cytosolic subunits and two membrane-bound subunits: a gp91phox and p22phox make up the catalytic core of the complex. The NOX is responsible for catalyzing superoxide from molecular oxygen, where NADPH component acts as the electron donor. Figure 1.6 was drawn using by BioRender.

1.4.2. The NADPH oxidases in atherosclerosis development

The amount of NOX expression is low in normal physiological states. However, there is evidence of a significant increase of NOX expression when the cells are subjected to hyperlipidemia, high glucose levels, and mitogenic or transforming growth factors. These stimuli lead to an overproduction of ROS and promote oxidative stress development [64, 65]. The level of NADPH oxidase expression determines the level of ROS production. The activation of NOX includes phosphorylation-dependent pathways. Studies have confirmed that the epigenetic regulation of NOX expression includes the presence of non-coding RNAs, deoxyribonucleic acid (DNA) methylation, variations of transcriptional factors activity, regulation of mRNA stability, and post-translational modification of histones [66]. Hence, the regulation of NOX expression depends on various factors that regulate the formation of ROS level in the body.

Many studies have shown that NOX homologues participate in numerous crucial roles in atherogenesis, as upregulation of its expression was demonstrated in CVD [67]. NOXs contribute to atherosclerosis pathogenesis, as their function includes endothelial dysfunction, vascular inflammation, vascular remodeling, and oxidative stress, where oxidative stress is a crucial component of the atherosclerosis progression. Studies confirm that oxidative stress by ROS results in oxidative modification of LDL and studies observed ROS produced by NADPH oxidases played a main role in the stimulation of early autophagy [68]. Therefore, NOX-mediated ROS has been linked to many stages of atherosclerosis pathogenesis.

Evidence demonstrated that NOX1 and NOX2 enzymes have pro-atherogenic activities, as the overexpression of NOX1 was evident in patients with CVD in comparison to atherosclerotic lesions of healthy humans [69, 70]. Furthermore, animal models lacking NOX2 exhibited reduced atherosclerosis in the descending aorta but did not reduce the atherogenesis in the aortic sinus [71].

NOX4 generates hydrogen peroxide because of the dismutation of superoxide. Unlike superoxide, hydrogen peroxide does not produce peroxynitrite, a strong oxidant showing a varied range of tissue damaging effects, as well as lipid peroxidation and inhibition of mitochondrial respiration [67]. The NOX4-mediated hydrogen peroxide showed an athero-protective role, as it reduced the rate of proliferation of vascular smooth muscle cells (VSMCs), inhibiting vascular inflammation and retaining heme oxygenase-1 (HMOX1) expression and eNOS in cases of any vascular stress [72, 73]. The NOX4-mediated ROS due to ox-LDL when exposed to monocytes and macrophages was shown to trigger cell death. Furthermore, damaging effects from NOX4 were observed in various rodent models that displayed ischemic stroke and cardiac hypertrophy [74]. However, there are studies where NOX4 enzymes showed anti-atherosclerotic activity [71, 74]. Hence, NOX4 enzymes can be atherogenic or athero-protective depending on their expression on differentcell types, the quantities of compound secreted, and their subcellular site. In the rodent genome, NOX5 is not present, making it difficult to study. However, in the intima of advanced coronary lesions, as well as early stages of endothelial lesions in humans, NOX5 expression was observed. NOX5 has been linked to human hypertension [75, 76]. Furthermore, incidence of oxidative damage is confirmed by the calcium dependent NOX5, as it is a crucial source of ROS in atherosclerosis. In addition, evidence of *NOX5* RNA and proteins in coronary arteries were expressed at significantly higher quantities in those patients with coronary heart diseases compared to healthy arteries, which was directly proportional to the calcium-dependent NOX activities in arteries [75]. Therefore, the overexpression of NOX1, NOX2, and NOX5 is atherogenic, whereas NOX4 shows both athero-protective and atherogenic properties depending on cell types.

1.5. The small nucleolar RNA

Small nucleolar RNAs (SnoRNAs) are medium-sized, 60–300 nucleotides in length, non-coding RNAs that are usually encoded in the introns of the host genes [76,77]. These host genes transcribe most of the snoRNAs in the nucleus. The primary transcripts consisting of the pre-mRNA of introns are then subjected to splicing, debranching, and trimming, and finally the mature snoRNAs are delivered to the nucleolus. Most function by guiding post-transcriptional modifications and processing of ribosomal RNA (rRNA) and some spliceosomal RNAs [77-80]. Few snoRNAs have been reported being involved in subjecting the original rRNA transcript to nucleolytic processing [81–85]. These post-transcriptional modifications are of prime importance for generating correct and functional ribosomes [86]. Thus, snoRNAs are required for guiding rRNA post-transcriptional modification and processing.

Based on their distinctive structural features, snoRNAs consist of two major categories: box C/D snoRNAs and box H/ACA snoRNAs [87].The name box C/D snoRNA was named for its two conserved motifs, box C accounts for the nucleotide sequence RUGAUGA and box D contains nucleotide sequence CUGA at the 5'-terminiand 3'-termini, respectively [88]. Furthermore, it has a "K-turn" structure, which assists associated core proteins to form small nucleolar ribonucleoproteins (snoRNPs) [78,89]. The complex of coreproteins on snoRNAs is expected to shield mature snoRNAs from exonucleolytic trimming [90]. On the other hand, box H/ACA snoRNAs have a "hairpin-hinge-hairpin-tail" structure [87, 88], where box H has a nucleotide sequence of ANANNA and boxes ACA accounts for nucleotide sequence ACA [91, 92]. The structure of the snoRNA is crucial to how they perform their functions.

The C/D box snoRNAs elucidate the target sites for 2′-O-ribose methylation, whereas H/ACAbox snoRNAs elucidate the target sites for pseudouridylation in the target RNA. C/D box

snoRNA and H/ACA box snoRNAs vary in their final structures, where their distinctive features make themable to bind to specific proteins to form snoRNP complexes that help in altering the relevant targets. The guide sequence of snoRNA hybridizes accurately to the target sequence in the rRNA, and the protein complexes connected to it then accomplish the relevant modification recognized by the snoRNAs on the nucleotide of rRNA. For processing rRNA, modification by thesesnoRNAs and their sites play a vital role. A defect in their modification or location may result in problems with rRNA processing and having an overall negative impact on cell growth [93]. Henceforth, abnormalities with snoRNA may be playing role in diseases, including CVD.

1.6. Objectives

Our laboratory previously reported that lipid HPs from total Lp by LPL caused the upregulation of 63 snoRNA transcripts. Additionally, our laboratory found the amount of 18S and 28S RNA was decreased due to upregulation of snoRNA, displaying a hallmark of macrophage to foam cell conversion [94]. Previously, Holley *et al.* [95] reported that cytosolic snoRNA levels within H9c2 rat cardiomyocytes were significantly increased under doxorubicin-induced ROS. Moreover, Wang *et al.* [96] reported that VLDL HPs generated by LPL induced ROS production in human aortic endothelial cells (HAEC), which was attenuated by NOX inhibitors (NOXi).

Thus, taken together with our laboratory's previous data and the above studies as my study rationale, my aim was to assess the oxidative stress induced in THP-1 macrophages when subjected to Lp HPs by LPL and to determine if NOXi could improve the oxidative stress condition in THP-1 macrophages. To address this aim, my thesis objectives were:

1) To measure the change in ROS production in THP-1 macrophage cells in response to HPs by LPL, with and without NOXi;

2) To measure the change in malondialdehyde (MDA) in THP-1 macrophage cells in response to HPs by LPL, with and without NOXi; and

3) To carry out *in silico* analyses to find common differentially expressed genes (DEG) that change within different cell lines in response to Lp HPs by LPL.

I expect that both ROS and MDA will be increased when macrophages are treated with Lp HPs by LPL, causing oxidative stress and that NOXi will reduce the oxidative stress. I further anticipate that changes in stress-related gene expression will be observed in different cell lines due to the Lp HPs by LPL in the bioinformatics study.

1.7. Hypothesis

I hypothesized that Lp hydrolysis products produced by LPL lead to NOX-mediated oxidative stress within macrophages that can be inhibited using NOXi. I further hypothesized that stress-related gene expression will increase due to Lp HPs by LPL in different cell lines.

1.8. Significance

LPL expression in macrophages promotes atherosclerosis. Previous studies from our laboratory have shown that Lp HPs that are generated by LPL alter gene transcription and cell signaling pathways that could impact the cellular functions of macrophages. This study will determine if NOX is an effector of Lp HPs-mediated ROS and MDA production. Understanding the role of NOX and the impact of the LPL HPs on atherosclerosis will potentially highlight macrophage LPL as a therapeutic target in the future. Moreover, the *in silico* study will provide information on shared gene expression among cell lines related which have been treated with Lp HPs generated by LPL. These genes can be targeted and manipulated in the wet lab in the future to find more insights in the role of macrophage LPL on foam cell formation.

Chapter 2: Materials and methods

2.1. Mammalian cell culture

2.1.1. HEK-293 cell culture and maintenance

Human embryonic kidney (HEK-293) cells were purchased from the American Type Culture Collection (ATCC). The cells were grown with Dulbecco's Modified Eagle Medium (DMEM) growth media comprising of 4.5 g/L glucose, 3.7 g/L sodium bicarbonate, 584 mg/L L-glutamine, and 110 mg/L sodium pyruvate (#SH30243FS, Fisher Scientific) in T75 culture flasks (#C353136, Corning Life Sciences). The medium was further supplemented with 1% v/v antibiotic/antimycotic (A/A) (#15240062, Invitrogen) and 10% v/v fetal bovine serum (FBS) (#A7906-100G, Sigma-Aldrich-Aldrich) with a pH ranging 7.2-7.4. The HEK-293 cells were incubated at a temperature of 37°C with 5% $CO2_{(g)}$. When the cells reached about 80-90% confluency, the old medium was discarded, and the cells in the flask were washed carefully with 4 mL of non-supplemented DMEM medium. After washing, the cells were treated with 2.5 mL of 0.25% (w/v) trypsin-ethylenediaminetetraacetic acid (EDTA) (#25200056, Fisher Scientific) and were incubated for 2 minutes at 37°C for the cell detachment from the flask surface. Following incubation, the spent trypsin was discarded and 14 mL of supplemented DMEM growth medium was added to the flask for forming a cell suspension by mixing with pipetting.Finally, 1 mL of the cell suspension was transferred to a new T75 flask containing 14 mL of fresh DMEM growth medium and incubated at a temperature of 37˚C with 5% $CO2(g)$.

2.1.2. THP-1 monocyte cell culture and differentiation

THP-1 monocytic cells (ATCC) were grown with Roswell Park Memorial Institute (RPMI)-1640 media comprising of 25 mM HEPES and 0.3 mg/L L-glutamine (#SH30255.01,HyClone) in T75 culture flasks (#C353136, Corning Life Sciences). The

medium was further supplemented with 1% v/v A/A (#15240062, Invitrogen) and 10% v/v fetal bovine serum (FBS) (#A7906-100G, Sigma-Aldrich-Aldrich), and the cells were incubated at a temperature of 37°C with 5% CO2(g). After 4 days of incubation, 3 mL (8×10^5 cells/mL) of the cell suspension was transferred to a new T75 flask containing 12 mL of supplemented RPMI-1640 growth medium, and cells were incubated at a temperature of 37˚C with 5% CO2(g).

For differentiating THP-1 cells, when the cell concentration reached 8×10^5 cells/mL, the cell suspension was transferred to a 15 mL centrifuge tube and spun down at 200 *g* for 5 minutes. Following centrifugation, the supernatant was discarded carefully and 5 mL of conditioned medium RPMI-1640 was added to the cell pellets and mixed thoroughly. The cells were counted with a hemocytometer and 100 µL of 1 × 104 cells/mL were added to dark, clear-bottom 96-well microplate for ROS assay (see *section 2.6.1*) with 100 nM of phorbol 12-myristate-13-acetate (PMA) (#79346, Sigma). Whereas 2.5 mL of 1 x 10^6 cells/mL was added with 100 nM of PMA in clear 6 well plates for thiobarbituric acid reactive substance TBARS assay (see *section 2.6.2*). After 48 hours of incubation of cells with PMA, the cells were washed three times with RPMI-1640 without FBS and A/A, and then incubated with RPMI-1640 media containing 0.2% w/v fatty acid free-bovine serum albumin (#A7906-100G ,FAF-BSA) (Sigma), 1% v/v A/A, and 100 nM PMA. After 24 hours of incubation, the cells were washed once with RPMI-1640 media and incubated for 1 hour by supplementing RPMI-1640 media with 0.2 % w/v FAF-BSA, 1% v/v A/A, 100 nM PMA and 25 µg/mL tetrahydrolypstatin (THL) (#O4139, Sigma-Aldrich) dissolved in dimethyl sulfoxide (DMSO) (#276855, Sigma- Aldrich). The THL was added to the cells to inhibit any endogenous lipase activity.

2.1.3. Cell counting and cell seeding using trypan blue exclusion assay

The number of viable cells, before treatment with LPL HPs or non-HPs, was assessed using Trypan Blue. Briefly, the monocyte cells after 4 days of sub-culturing were placed into a 15 mL centrifuge tube. The cells were centrifuged at 200 g for 5 minutes and the supernatant was removed. Following supernatant removal, the cell pellets were mixed thoroughly with 5 mL of RPMI media supplemented with 10% FBS and 1% A/A (see *section 2.1.2*). In a separate microfuge tube, 30 µL of cell suspension was mixed with 30 µL of 0.4% (w/v) trypan blue (#25-900-CI, Corning). The cells were then loaded into a hemocytometer and live cells were counted in a specified area under the microscope. The following formula was used to calculate cell seeding density in cells per mL:

$$\text{Seeding Density} = \frac{\textbf{Cells in four quadrants}}{\textbf{4}} \times \mathbf{2 \times 10^4}$$

2.2. HEK-293 transfection with recombinant LPL plasmid

2.2.1. HEK-293 cell transfection

HEK-293 cells at 70-80% confluency in T75 flasks were washed with 4 mL non-supplemented DMEM and treated with trypsin (per *section 2.1.1*). After separation of cells from the flask surface, 21 mL supplemented DMEM growth medium was added and mixed to the cell suspension, from which 10 mL of cells were seeded in two 10 cm cell culture dishes. For 24 hours, the cells were incubated at 37°C with 5% CO_2 (g). Following incubation, cells were transfected with Lipofectamine™ transfection reagent (#11668027, Fisher Scientific) and Opti-MEM reduced serum media (#31985070, ThermoFisher Scientific) containing 5.85 µg of pcDNA3.LPL plasmid or without plasmid (control)

[128]. The pcDNA3.LPL plasmid was generated using pcDNA3 containing the human LPL cDNA [GenBank:NM_000237] (pcDNA3.LPL, a gift from Dr. Daniel Rader, University of Pennsylvania, Philadelphia, PA, USA) using *Escherichia coli* DH5α competent cells (#60602-1, Lucigen). Previous data from our laboratory report no changes in the activity of lipase between transfected control cells with an empty pcDNA3 vector and transfected cells withno vector [94]. After a 5 hour incubation period, 5.8 mL supplemented DMEM growth medium with 20% v/v FBS and 2% v/v A/A was added to the cells and incubated for 19 hours at 37°C with 5% CO_2. Following the incubation period, the cells were washed using 5 mL of DMEM andwere treated with 5 mL of heparinized DMEM containing 1% v/v A/A and 10 U/mL heparin (# C504710, Organon) for 23.5 hours at 37°C with 5% CO_2 . Addition of heparin allows the medium to contain the LPL, as heparin displaces LPL from the cells to the medium. After incubation, cells were then treated with 1 mL of heparinized DMEM containing 100 U/mL heparin and 1% v/v A/A and were incubated for 30 minutes at 37°C with 5% CO_2(g). In 15 mL centrifuge tubes, media from both plates containing control and LPL were centrifuged to remove the cell debris. Finally, LPL-containing media and control media were aliquoted in 1.5 mL tubes and stored at -80˚C until use.

2.3. Qualitative and quantitative analysis of LPL

2.3.1. LPL activity assay

LPL activity was assessed using 1, 2-*O*-dilauryl-*rac*-glycero-3-glutaric-resorufin ester (#D7816-10MG, Sigma) as substrate, as previously described by Lehner *et al*. [84]. In brief, 2 mg of resorufin ester was added in 1 mL of dioxane (Sigma) to prepare a resorufin ester stock; the stock was stored at 4˚C until needed. In triplicate, 15 µL of heparinized media having LPL orcontrol media acquired from transfected HEK-293 cells (see *section 2.2.2*) was mixed with 165 µL of a lipase assay buffer (20 mM Tris, 1 mM EDTA, pH 8.0) in a clear, lidless and non-sterile 96 well plate (#12565226, ThermoFisher Scientific). Next, the lipase assay buffer was added as a diluent to 20 µL resorufin ester to yield a 0.3 mg/mL concentration, which was added to each sample well containing LPL or control media (15 µL of heparinized media having LPL/ control media and 165 µL of a lipase assay buffer). The absorbance of the plate was read at 572 nm over 60 minutes at 25˚C using a Synergy Mx fluorescent plate reader (Bio-Tek). The standard curve was obtained by dilution of 400 µM resorufin ester stock in 200 µL lipase assay buffer to 0, 1, 2, 3, 4, 6, 10, 15, 20, 40 µM concentrations. Using that standard curve, the rate of concentration of resorufin released was determined, where the linear portion of the kinetic graph was used to plot the bar chart activity of LPL and control samples.

2.3.2. SDS-PAGE and immunoblot analysis

Heparinized media from LPL-expressing (or control) cells were analyzed by sodium dodecyl sulfide polyacrylamide gel electrophoresis (SDS-PAGE) to investigate if LPL transfections were successful. A 10% w/v resolving gel and a 4% w/v stacking gel was prepared from a stock solution of 30% acrylamide:*bis*-acrylamide (#A3574, Sigma-Aldrich). A total of 37.5 µL of heparinized media was mixed with 12.5 µL of 4x a sample lysis buffer (50% v/v

glycerol, 6% v/v β-mercaptoethanol, 10% w/v SDS, and 0.01% w/v bromophenol blue). The mixture was boiled at 100°C for 6 minutes. Following boiling, 20 µL of each sample was loaded into the SDS-PAGE gel. The gel ran for 45 minutes at 200 V, using a running buffer that consists of 1X Tris-glycine-SDS (TGS) solution with a pH of 7.4 diluted from 10x TGS containing 25 mM Tris, 192 mM glycine, and 0.1% SDS (#1610772, Bio-Rad). The proteins were transferred using an ice-cold transfer buffer of TGS with 20 % v/v methanol (#A456-4, ThermoFisher Scientific) onto a nitrocellulose membrane (#1620115, Bio-Rad) at 300 mA for 3 hours at 4˚C. Following the transfer, a blocking solution of 5% w/v bovine serum albumin (BSA) (#A7906, Sigma-Aldrich), 0.05% v/v Tween-20 (#P9416, Sigma-Aldrich), and 0.05% w/v sodium azide (ThermoFisher Scientific) in 1X Tris-buffered saline (TBS) (which is prepared from 10x premixed electrophoresis buffer containing 25 mM Tris, 192 mM glycine) at pH 7.4 was incubated with the membrane at 4°C overnight on a rocking platform. Next, the blocking solution was replaced with a 1:2,000 dilution of a polyclonal anti-human LPL antibody (#sc- 32885, Santa Cruz Biotechnology, Santa Cruz, CA, USA) in 5% BSA, then incubated overnight with rocking at 4°C. Th next day, the membrane was washed four times for 10 minutes

with 15 mL of TBS containing 0.05% v/v Tween-20 in a rocking platform. The membrane was then incubated with secondary antibody with 1:2,000 dilution of a horseradish peroxidase-conjugated anti-rabbit IgG (#SA1-200, Pierce Biotechnology, Rockford, IL, USA) in 5% BSA, incubated for 2 hours with rocking. Following incubation, the membrane was washed 4 times with TBS containing 0.05% v/v Tween-20 for 10 minutes each while rocking. Lastly, for the protein visualization, the membrane was treated with the ECL^{TM} Western Blotting Detection Kitsolution (#RPN2232, GE Healthcare), according to manufacturer's instructions. The ImageQuant

`

4000 gel imager (GE Healthcare) was used to detect the chemiluminescence, and ImageJ software for semi-quantifying the protein bands formed in the image.

2.4. Lipoproteins

Human VLDL (cat. #365-10, Lee Biosolutions), with a triglyceride content of 11,740 mg/dL and total cholesterol of 3,360 mg/dL; and human CM (cat. #194-14, Lee Biosolutions), with a TG content of 8,580 mg/dL and total cholesterol of 670 mg/dL; were purchased and stored at -80°C until needed.

2.5. Lipoprotein HPs generation, quantification, and incubation with THP-1 macrophages

2.5.1. Lipoprotein hydrolysis by LPL

The VLDL and CM Lps (see *section 2.4*) were diluted with PBS to 1:16 of its original concentration. The dilution of Lp should have been carried out with supplemented RPMI instead of PBS to avoid cell nutrient deprivation. The diluted Lp was further mixed with heparinized media containing LPL or control in 1:1 ratio to generate Lp HPs. The mixtures were then incubated at 37°C for 4 hours and, right after incubation, they were put on ice. The quantification of FFA liberated from the Lps were determined (see *section 2.5.2*). Finally, the Lp HPs by LPL or control were used promptly to incubate THP-1 macrophages (see *section 2.5.3*).

2.5.2. FFA quantification from lipoprotein HPs

The measurement of total FFA produced from Lp lipid hydrolysis by LPL was carried out using the non-esterified free fatty acid (NEFA)-HR (2) commercial kit (Wako) per manufacturer's instructions. In brief, 4 μL of LPL HPs or non-HPs were added to a well in a clear, lidless, and non-sterile 96 well plate (#12565226, ThermoFisher Scientific). From the kit, 225 μL of Solvent A was added to the sample well and the plate was then incubated for 10

minutes at 37˚C. After incubation, 75 µL of Solvent B was added to the samples, which were incubated at 37˚C for another 10 minutes. The Synergy Mx fluorescent plate reader was used to measure the samples with absorbance of 550 nm at 37˚C. A standard curve was obtained from a NEFA stock solution within the kit, containing 1 mM oleic acid, which was diluted to 0, 0.5, 0.75, 1, 1.5, 2, or 4 µL with distilled H_2O to reach a final volume of 4 µL in each well. Solutions A and B were then used, as above. The standard curve was used to find the concentration of FFAin each sample having HPs and non-HPs.

2.5.3. THP-1 macrophage treatment with lipoprotein HPs

Using Lp HPs were added to differentiated THP-1 cells (*see section 2.1.2*). At 48 hours of differentiation, cells were washed three times with plain RPMI-1640 and then incubated with RPMI-1640 supplemented with 0.2% w/v FAF-BSA, 1% v/v A/A, and 100 nM PMA for 24 hours at 37°C with 5% CO_2 (g). Following 24-hour incubation, the cells were subjected to 1 hour pre-treatment with the fatty acid-free medium solution comprising of 0.2% FAF-BSA, 1% A/A, 100 nM PMA, and 25 µg/mL THL. During this time, Lp HPs generated by LPL were diluted to 0.25, 0.5, and 0.75 mM concentration with the fatty acid medium solution described above. Heparinized media from control-transfected cells, diluted to mimic the diluted volumes from LPL-containing media, were also prepared. Following the pre-treatment, the spent media from the cells was removed and LPL HPs or non-HPs with or without 100 µm of NOXi, apocynin (#178385-1GM, Sigma-aldrich) diluted in DMSO were added to the THP-1 macrophage cells in triplicate for 24 hours treatment period at 37°C.

2.6. Analysis of THP-1 macrophage cell oxidative stress

2.6.1. Measurement of ROS with ROS assay

ROS formation by THP-1 macrophages in the absence or presence of HPs over 24 hours (*see section 2.5.4*) in a 96 well plate was quantified using the DCFDA / H2DCFDA - Cellular ROS Assay Kit (ab113851, Abcam). Four hours prior to completion of the 24-hour treatment, 100 µL of 500 µM *tert*-butyl hydroperoxide (TBHP) was diluted with 9 parts 1X Buffer to 1 part FBS, were added to three wells, as positive controls provided with the kit, and incubated the plate at 37°C for 4 hours. At 45 minutes prior to the completion of the 24-hour treatment, 100 µL of 25 µM DCFDA diluted with RPMI-1640, with L-glutamine, no phenol (#11835030, ThermoFisher Scientific), supplemented with 0.2% FAF-BSA, 1% A/A, 100 nM PMA, and 25 µg/mL THL, was added to all the cells and incubated at 37°C for 45 minutes and wrapped with aluminum foil to avoid light. Following that, the supernatant was transferred from each well to new wells of the dark, clear bottom 96 well plate. The plate containing both media and cells was measured immediately using Synergy Mx fluorescent plate reader at Ex/Em = 485/535 nm in end point mode with auto gain. Blank well intensity was subtracted from each sample's fluorescence to give the corrected fluorescence intensity for each sample. The corrected fluorescence intensity is proportional to ROS production. Following reading, the plate containing the cells were treated with 0.1 M NaOH for 30 minutes at room temperature for cell lysis. Following 30 minutes, the protein concentration of the cell lysates was determined using bicinchonic acid (BCA) (see *section 2.6.3*). The ROS production was normalized by the protein concentration of each well.

2.6.2. Measurement of MDA with TBAR assay

The quantification of MDA formation from the THP-1 macrophage cells and media after a 24- hour treatment with hydrolysis or non-HPs in a 6 well plate was carried out using a TBARS Parameter Assay Kit (#KGE013, R&D Systems Inc.). After 24 hours of treatment, the media were collected and stored at -80°C until further use. After collection of the media, the cells were washed with cold PBS and then were resuspended at 1 x 10^6 cells/mL in the cell lysis buffer 3 (#895366, R&D Systems Inc.), diluted 5-fold with distilled water. Following addition of buffer, cells were incubated with gentle agitation for 30 minutes at 4 °C. After 30 minutes, the cells were stored at ≤-20 °C until further use.

For carrying out the TBARS assay in the cell and media samples, firstly, MDA stock was generated. To prepare it, 100 µL of TBARS Standard was added to 200 µL of TBARS acid reagent (provided with the kit) and kept at room temperature with gentle agitation for 30 minutes to produce167 µM MDA stock solution. After 30 minutes, the MDA stock solution was diluted to 8.35, 4.18,2.09, 1.04, 0.52, 0.26 and 0 µM concentration with deionized water. Using that standard curve, concentration of MDA formed in the cells and media samples were determined.

Secondly, for sample preparation, 300 µL of each sample was treated with 300 µL TBARS acidreagent in microfuge tubes and incubated for 15 minutes at room temperature. After 15 minutes, the microfuge tubes were centrifuged at ≥ 12,000 × *g* for 4 minutes and the supernatant was collected for the TBARS assay.

Finally, in triplicate, 150 µL standards and samples were loaded to each well of the microplatestrips provided with the kit and 75 µL of thiobarbituric acid (TBA) reagent were added to the standard and sample wells. The pre-optical density was taken of each well using Synergy Mx. fluorescent plate reader set to 532 nm absorbance and 37°C. The microplate was

then covered withthe adhesive strip provided and was incubated for 3 hours at 47 °C. Following 3 hours, the final optical density of each well was determined at 532 nm absorbance and at a temperature of 47 °C.The pre-reading was then subtracted from the final reading to determine sample MDA formation. The protein concentration was determined using BCA (see section 2.6.3), for normalization of sample MDA formation.

2.6.3. BCA assay

The protein concentration of cell lysate was carried out using a BCA Protein Assay kit (#PI23235, Fisher Scientific), following the manufacturer's instructions. The standard of albumin at 0, 25, 125, 250, 500, 750, 1,000, 1,500, and 2,000 mg/mL was diluted with 1X PBS for generating a standard curve.

In triplicate, 25 µL standards and samples were loaded to each well of a clear, without lid and non-sterile 96 well plate and 200 µL of BCA assay buffer were added to the standard and samplewells and was incubated at 37°C for 30 minutes. The plate was then read at absorbance 562 nm using a PowerWave XS microplate reader. The absorbance reading was corrected from the diluentabsorbance reading to calculate the protein concentration of the samples.

2.7. *In silico* analysis

Gene expression data from human macrophage (GSE84791) and astrocyte lines (GSE76696) were obtained from the Gene Expression Omnibus (GEO) database (GPL570-Affymetrix Human Genome U133 Plus 2.0 Array platform). The RAW file downloaded from the GEO database was converted to CEL file using PeaZip software and was uploaded at Transcriptome analysis console (TAC) 4.0. The TAC 4.0 was used to obtain and analyze the

differential gene expressions (DEGs) in two cell lines. The visualization features such as the Venn diagram allowed to view and analyze the common gene expression data when the cell lines were treated with LPL HPs.

2.8. Statistical analysis

In this study, only two sets of experiments (n=2) were carried out to measure resultant ROS and MDA level in THP-1 cells in response to VLDL and CM HPs by LPL with and without NOXi. The two sets of experiments thus do not provide statistical information. Thus, the resultant ROS or MDA changes were interpreted as potential increases or decreases, when the SD among samples did not overlap. For the triplicate studies (n=3), the unpaired Student's *t*-test or one-way ANOVA were performed. All data are shown as mean ± SD. The statistical significance was represented as follows: Not significant $P > 0.05$; * $P \leq 0.05$; ** $P \leq 0.01$; and *** $P \leq 0.001$.

`

Chapter 3: Results

3.1. Analyzing recombinant human LPL obtained using HEK-293 transfection

3.1.1. Immunoblot and activity assay of recombinant human LPL

The western blot analysis was carried out to confirm the presence of full-length human LPL protein after the LPL transfection in HEK-293 heparinized media. As expected, the existence of LPL was validated as a band was observed at 55 kDa in the LPL-transfected HEK-293 heparinized media lane and there was no band formation at the control-transfected HEK-293 heparinized media lane and blank lane (only distilled water) in the gel image obtained from the western blot analysis (Figure 3.1A). The immunoblot result confirmed successful transfection of LPL protein in the heparinized media.

To assess the catalytic activity of the recombinant LPL obtained, a resorufin ester substrate was used. The heparinized media containing the transfected LPL showed significantly higher hydrolytic activity in comparison to the control-transfected heparinized media, as anticipated. The lipase activity which is proportional to the rate of resorufin product formation, demonstrated LPL-transfected heparinized media having significantly higher ($p \leq 0.001$) lipase activity of 2.432 ± 0.120 μmol/mL/min, whereas control-transfected media showed an activity of 0.069 ± 0.008 μmol/mL/min, $p \leq 0.001$ (Figure 3.1B). These results confirmed that LPL was present due to the band formation at its molecular mass, 55 kDa, and the transfected LPL was active as the lipase activity was higher in comparison to the control. Thus, the LPL was functional in the heparinized media, which could be used to generate Lp HPs for later experiments.

A)

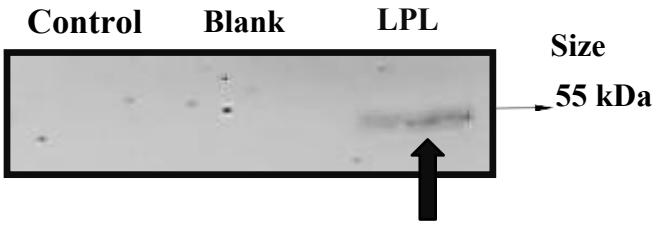

B)

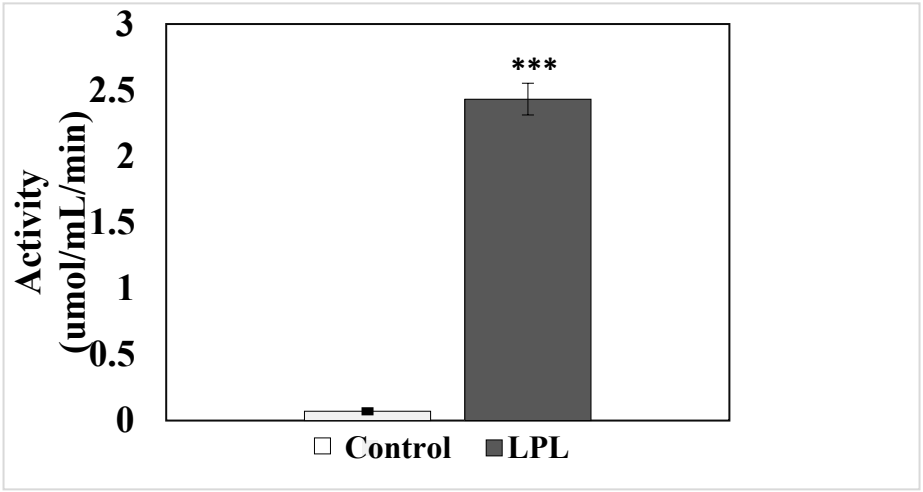

Figure 3.1: Assessment of protein expression and catalytic activity of recombinant LPL expressed in HEK-293 cells

HEK-293 cells were transfected with or without pcDNA3 including LPL cDNA. Both cell lysate and heparinized media were collected. **(A)** Immunoblot analysis of heparinized media from transfected cells were validated for LPL protein expression, where control was without LPL plasmid and blank was only distilled water. **(B)** The enzymatic activity of heparinized media taken from control and LPL-transfected cells was evaluated using a resorufin ester substrate. Data are presented as mean ± SD from triplicate experiments (n=3). Statistical analysis was performed using an unpaired *t*-test, $p \leq 0.001$ (***).

3.1.2. Hydrolysis of VLDL and CM lipoproteins by LPL

After the verification of active LPL, the Lps VLDL and CMs were diluted with PBS to 1:16 ratio of its original concentration and incubated with either heparinized media with no LPL or LPL transfected heparinized media for 4 hours at 37°C. As expected, the FFA amount generated from VLDL HPs by LPL (0.252 ± 0.002 nmol/µL) was significantly higher ($p \leq 0.001$) than VLDL treated with control (0.115 ± 0.009 nmol/µL) as shown in Figure 3.2A. Likewise, the FFA amount generated from CM by LPL (0.215 ± 0.005 nmol/µL) was significantly higher ($p \leq 0.001$) than its control HPs (0.132 ± 0.003 nmol/µL) as illustrated in Figure 3.2B. The HPs were then further diluted to concentration 0.25, 0.5 and 0.75 nmol/µL with RPMI-1640 media supplemented with 0.2 % FAF-BSA, 1 % A/A, 100 nM PMA, and 25µg/ mL THL dissolved in DMSO prior to being used to treat THP-1 macrophage cells. Moreover, the control cells were treated with the same concentration of the control HPs (0.25, 0.5 and 0.75nmol/µL).

(A)

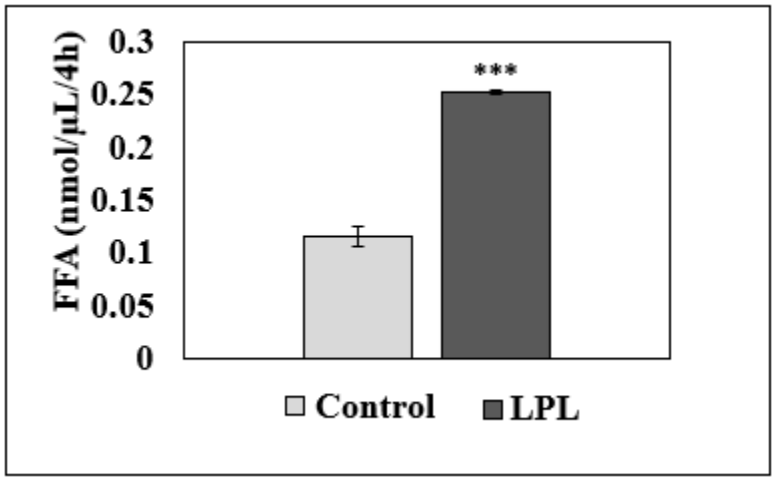

(B)

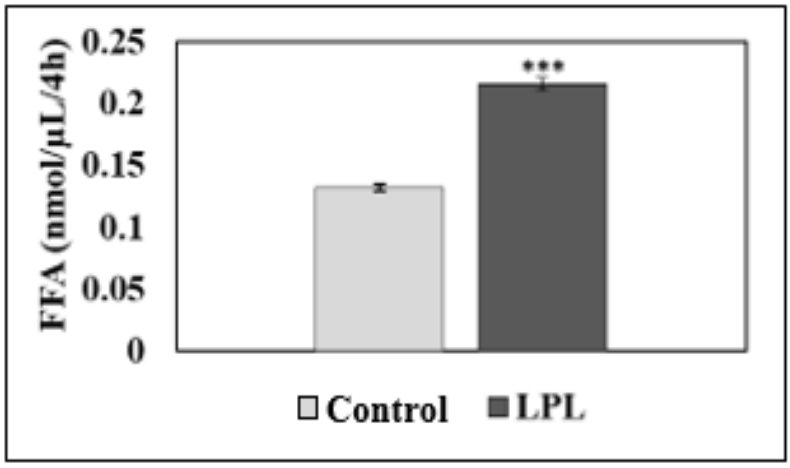

Figure 3.2: The amount of FFA formed in lipoprotein HPs after incubation with LPL or control-transfected heparinized media

LPL or control- transfected HEK-293 heparinized media were incubated with Lps for 4 hours at 37°C to generate HPs. The FFA content of the HPs was measured using the NEFA-HR (2) commercial kit according to manufacturer's instructions (*see section 2.5.2*). **(A)** The FFA generated from VLDL incubated with LPL or control- transfected HEK-293 heparinized media. **(B)** The FFA generated from CM incubated with LPL or control- transfected HEK-293 heparinized media. Data are presented as mean ± SD from triplicate experiments (n=3).

`

Statistical analysis was performed with an unpaired *t*-test, $p \leq 0.001$ (***) compared to control.

3.2. The effect of lipoprotein HPs by LPL with or without NOXi on the ROS production of THP-1 cells and media

In this study, we analyzed the amount of intracellular and extracellular ROS formed in THP-1cells when treated with VLDL and CM HPs generated by LPL or control-transfected HEK-293 heparinized media, with or without NOXi for 24 hours at 37 °C.

3.2.1. The effect of VLDL lipoprotein HPs by LPL with or without NOXi on the ROS production of THP-1 cells and media

One of the objectives of this study was to determine the effect of VLDL Lp HPs on ROS production by THP-1 cells, in the absence or presence of NOXi. The cells were cultured and treated for 24 hours with VLDL HPs generated by LPL or control heparinized media, as per *section 2.5.4*. The ROS production within the cells and media after 24-hour treatment was measured using ROS assay (*see section 2.5.5*). The ROS generation due to Lp HPs was compared as percent of control, where control was set to 100 %. Therefore, ROS formed in the cells or media below 100% indicated lower ROS generation in the sample compared to control and vice versa. The lysates of cells treated with 0.25, 0.5 and 0.75 nmol/µL FFA from VLDL HPs generated by LPL accounted for intracellular ROS values of 22.2 ± 26.02%, 35.5 ± 17.96% and, 883.6 ± 182.8%, respectively – all relative to the control. Hence, the intracellular ROS in THP-1 cells showed a potential decrease in ROS generation proportion to 0.25 and 0.5 nmol/µL concentration of FFA but a potential increase for 0.75 nmol/µL concentration of FFA when treated with VLDL HPs by LPL in relative to control (Figure 3.3). Moreover, the THP-1 cells incubated with 0.5 nmol/µL FFA of VLDL HPs without and with 100 µM NOXi. The ROS produced without and with 100 µm NOXi, showed a potential decreased in the intracellular ROS of 35.5 ±13.23% and 24.4 ± 9.92%, respectively, relative to the control (Figure 3.4).

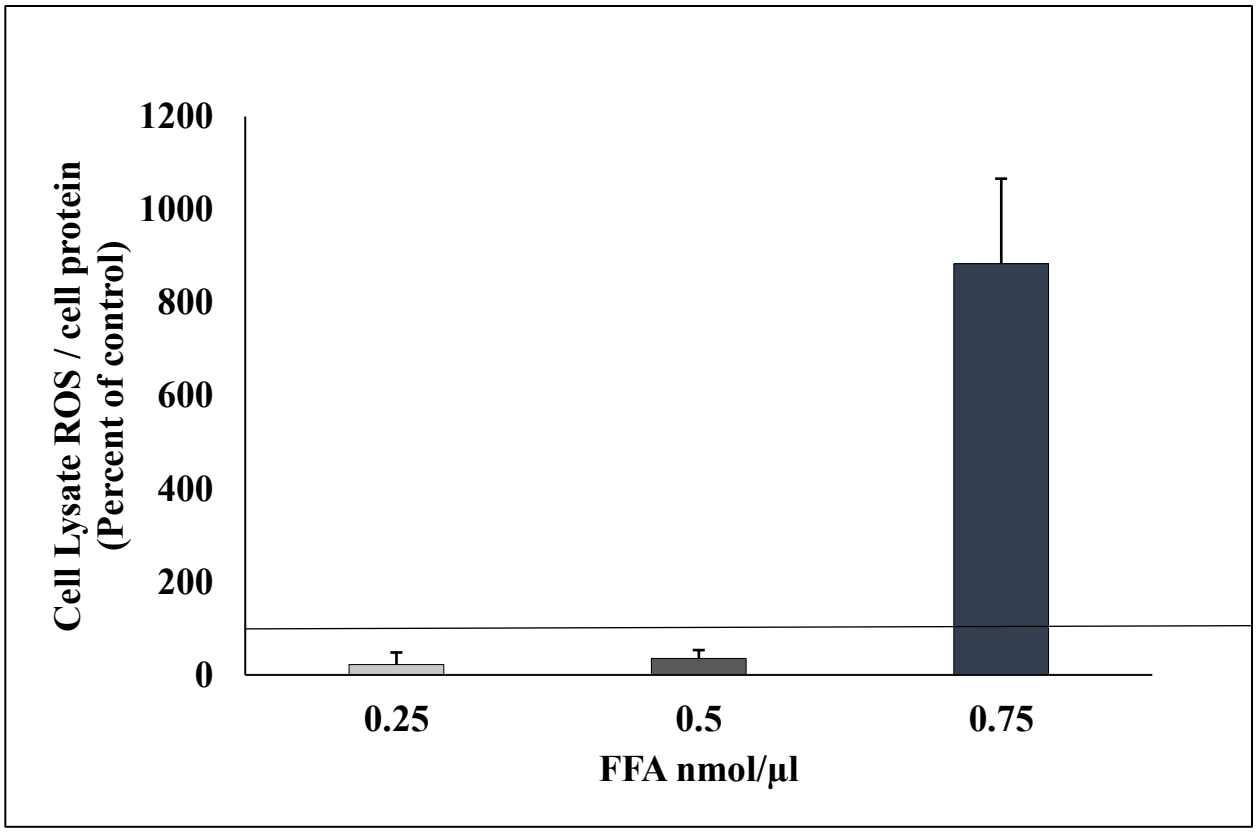

Figure 3.3: Intracellular ROS potentially decreased for the 0.25 and 0.5 nmol/µL FFA concentration but potentially increased with 0.75 nmol/µL FFA concentration liberated by VLDL HPs by LPL vs control

The THP-1 cells were treated with VLDL Lp HPs generated by LPL or control heparinized media for 24 hours at 37 °C. All the data are normalized with its protein concentration and presented as a percent of control with mean ± SD from duplicate experiments (n=2).

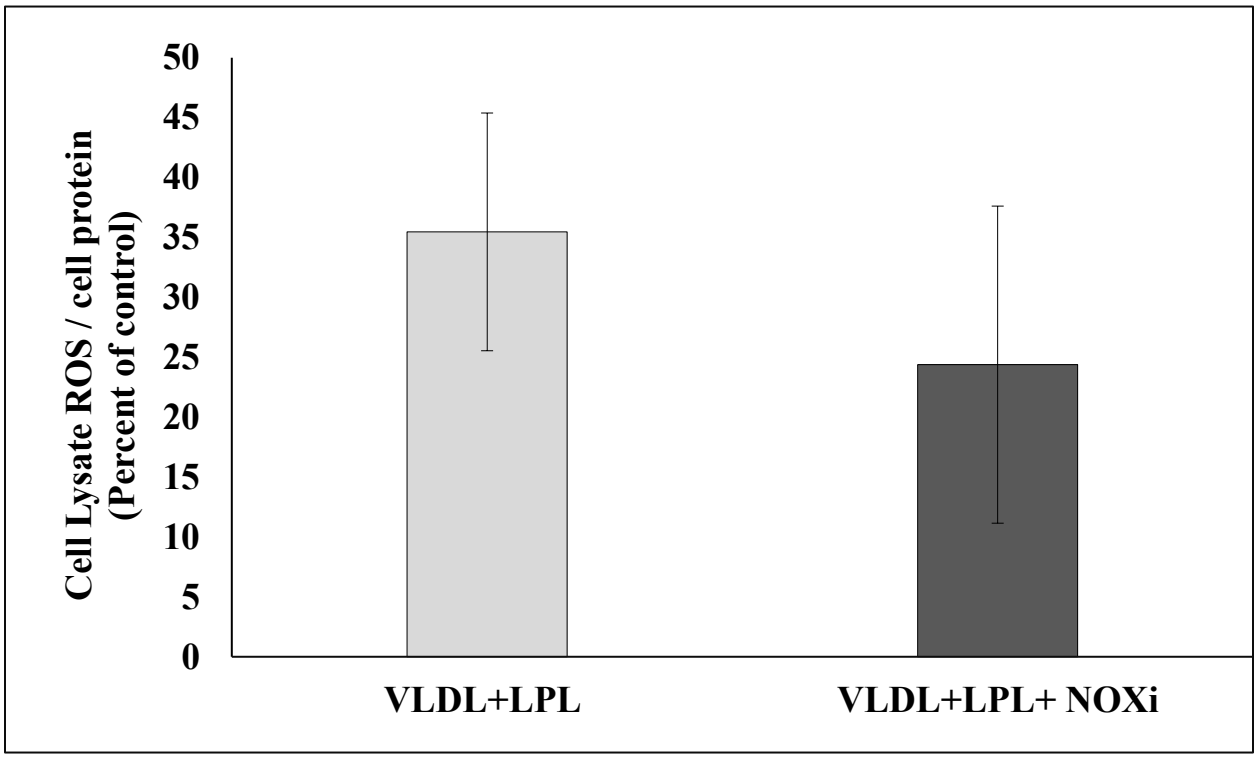

Figure 3.4: Intracellular ROS potentially decreased with VLDL HPs by LPL with and without NOXi treatment vs control

THP-1 cells were incubated with 0.5 nmol/µL FFA of VLDL HPs with or without 100 µM apocynin (NOXi) for 24 hours at 37 °C. All the data are normalized with its protein concentration and presented as a percent of control with mean ± SD from duplicate experiments (n=2).

`

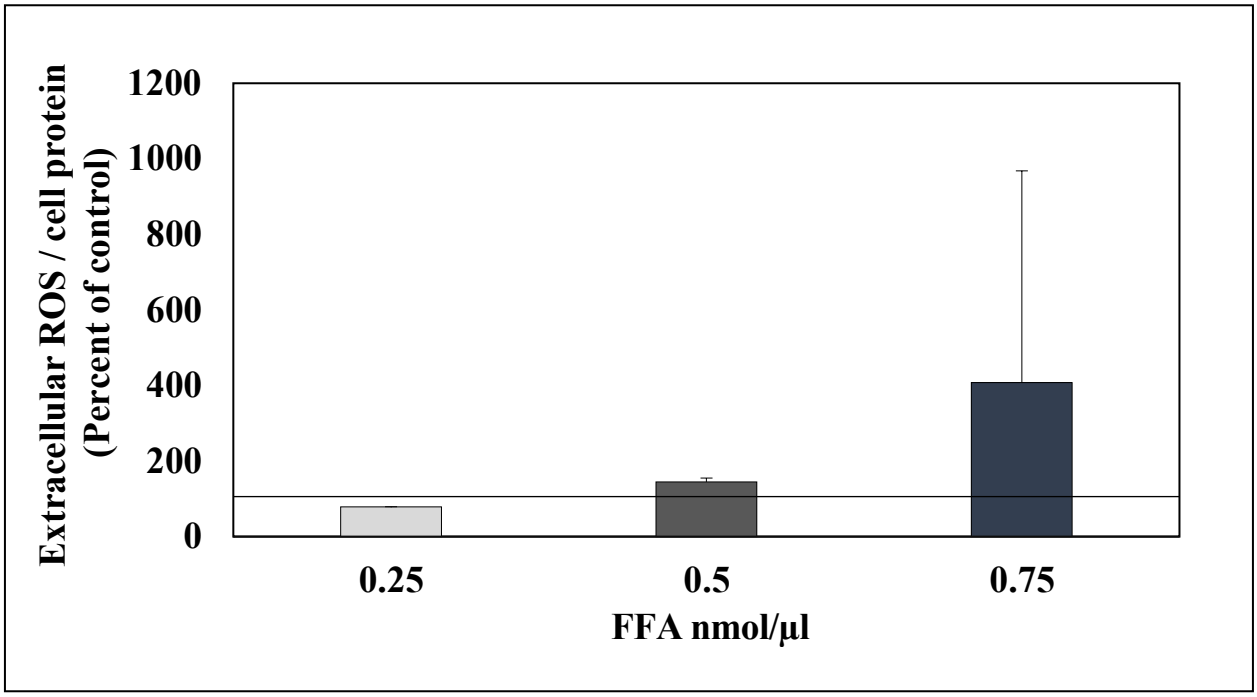

Figure 3.5: Extracellular ROS potentially decreased for 0.25 nmol/µLFFA concentration but potentially increases with 0.5 and 0.75 nmol/ µL FFA concentration liberated by VLDL HPs by LPL vs control

THP-1 cells were incubated with 0.25, 0.5 and 0.75 nmol/µL FFA mixture generated from VLDL HPs by LPL for 24 hours at 37 °C. All data are normalized with its protein concentration and presented as a percent of control with mean ± SD from duplicate experiments (n=2).

Thus, intracellular ROS reduces with VLDL HPs by LPL with and without NOXi treatment in comparison to control.

The media of cells treated with 0.25, 0.5 and 0.75 nmol/µL FFA from VLDL HPs generated by LPL accounted for extracellular ROS values of 78.4 ± 0.2%, 144.4 ± 10.06% and, 407.4 ± 560.5%, respectively, all relative to the control. Thus, the extracellular ROS proportion to the 0.25 nmol/µL concentration of FFA potentially decreased but for 0.5 nmol/µL and 0.75 nmol/µL concentration FFA fromVLDL HPs by LP, showed potential increasing in relative to control (Figure 3.5). Additionally, the THP-1 cells incubated with 0.5 nmol/µL FFA of VLDL HPs without and with 100 µm NOXi, showed a potential no change in the extracellular ROS of 144.4 ± 10.06% and 129.9 ± 13.5%, respectively, relative to the control (Figure 3.6).

`

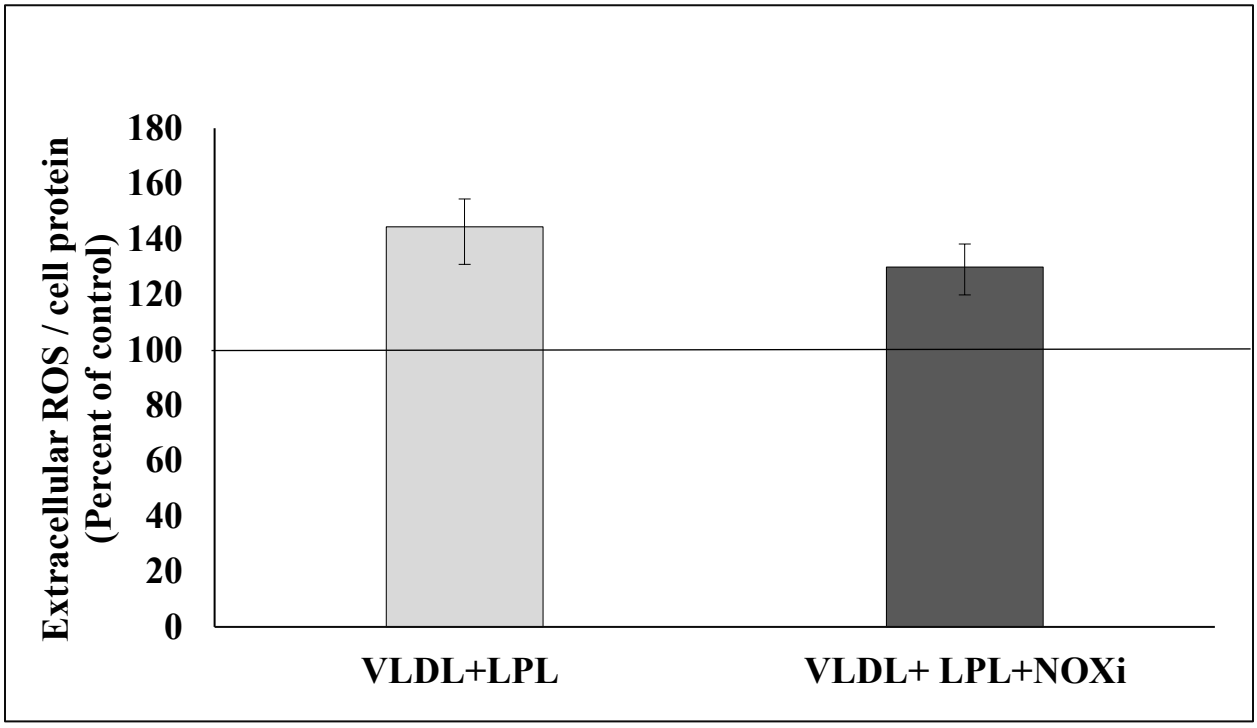

Figure 3.6: Extracellular ROS exhibiting potentially no change with VLDL HPs by LPL with and without NOXi treatment vs control

THP-1 cells were incubated with 0.5 nmol/µL FFA of VLDL HPs with or without 100 µM NOXi for 24 hours at 37 °C. All the data are normalized with its protein concentration and presented as a percent of control with mean ± SD from duplicate experiments (n=2).

3.2.2. The effect of CM HPs by LPL with or without NOXi on the ROS production of THP-1 cells and media

The next part of the study was to examine ROS levels in the THP-1 cells and media when treated for 24 hours with CM HPs liberated by LPL or control heparinized media, with or without NOXi. A trend similar to VLDL HPs by LPL was observed for intracellular ROS in THP-1 cells when treated with the HPs of CM by LPL or control. The lysates of cells treated with 0.25, 0.5 and 0.75 nmol/µL FFA from CM HPs generated by LPL accounted for intracellular ROS values of 32.8 ± 0.45, 26.02%, 84.2 ±3.68% and, 401.8 ± 317.5%, respectively – all relative to the control. Therefore, there was a potential decrease in intracellular ROS proportion to 0.25 and 0.5 nmol/µL concentration of FFA, whereas it increased for 0.75 nmol/µL concentration of FFA (Figure 3.7). Moreover, the THP-1 cells incubated with 0.5 nmol/µL FFA of CM HPs without NOXi potentially increased the intracellular ROS to 127.7% ± 26.71%, whereas with 100 µM NOXi, the intracellular ROS potentially decreased to 84.3% ± 7.49% – all relative to the control (Figure 3.8).

Furthermore, there was a potential decrease in extracellular ROS generation proportion to the 0.25 nmol/µL concentration of FFA but a potential increase for 0.5 and 0.75 nmol/µL concentration of FFA formed due to CM HPs by LPL in relative to control (Figure 3.9). The media of cells treated with 0.25, 0.5 and 0.75 nmol/µL FFA from CM HPs generated by LPL accounted for extracellular ROS values of 69.4 ± 22.1%, 127.7 ± 89.01% and, 346.1± 19.73%, respectively, all relative to the control. Moreover, the THP-1 cells incubated with 0.5 nmol/µL FFA of CM HPs without and with 100 µM NOXi showed a potential decrease in the intracellular ROS of 77.5 ± 26.7% and 53.6 ± 2.76% respectively, all relative to the control (Figure 3.10).

`

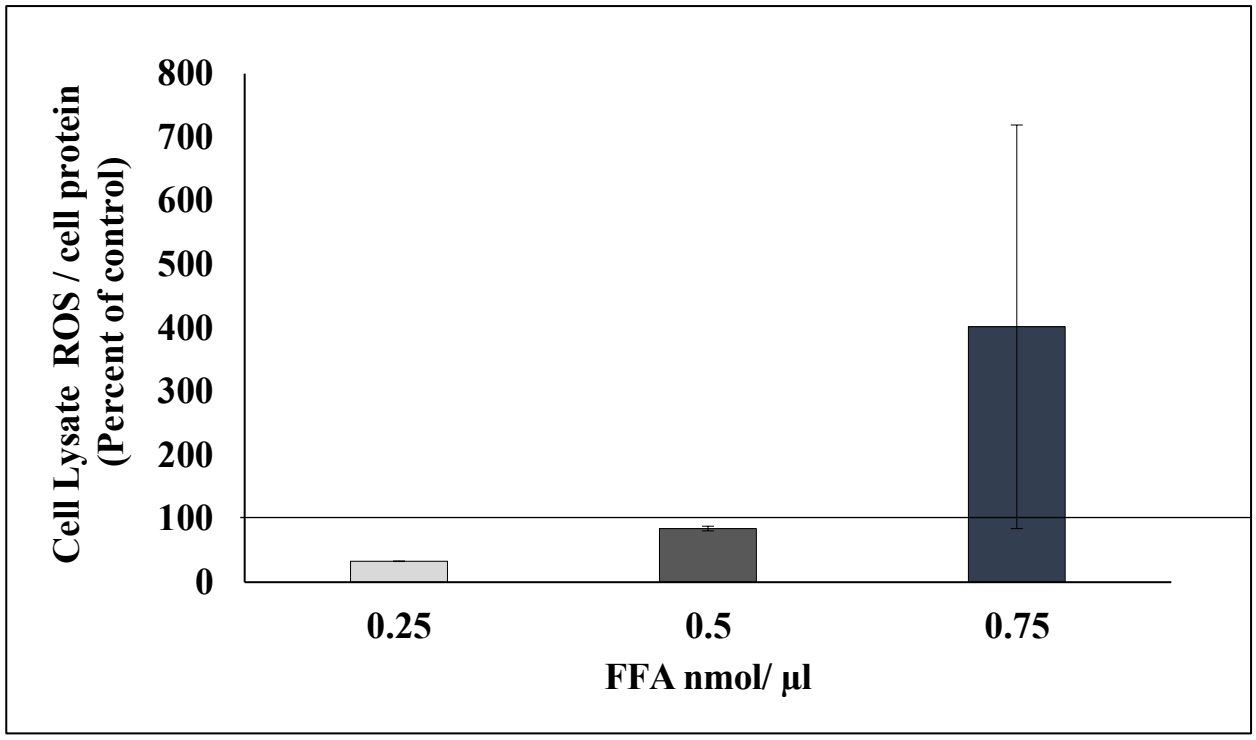

Figure 3.7: Intracellular ROS potentially decreased for the 0.25 and 0.5 nmol/µL FFA concentration but potentially increased with 0.75 nmol/µL FFA concentration liberated by CM HPs by LPL vs control

The THP-1 cells were treated with CM Lp HPs generated by LPL or control heparinized media for 24 hours at 37 °C. All data are normalized with its protein concentration and presented as a percent of control with mean ± SD from duplicate experiments (n=2).

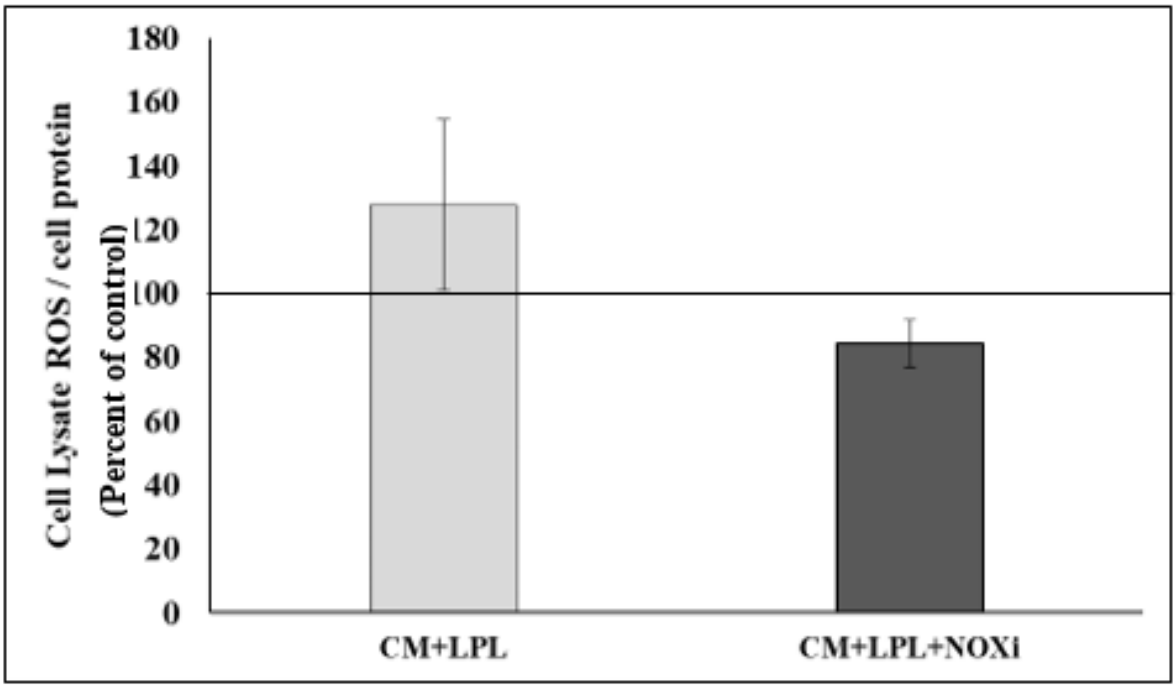

Figure 3.8: Intracellular ROS potentially decreased with CM HPs by LPL and NOXi treatment vs control

The THP-1 cells were incubated with 0.5 nmol/μL FFA from HPs of CM by LPL with or without 100 μM NOXi for 24 hours at 37 °C. All data are normalized with its protein concentration and presented as a percent of control with mean ± SD from duplicate experiments (n=2).

`

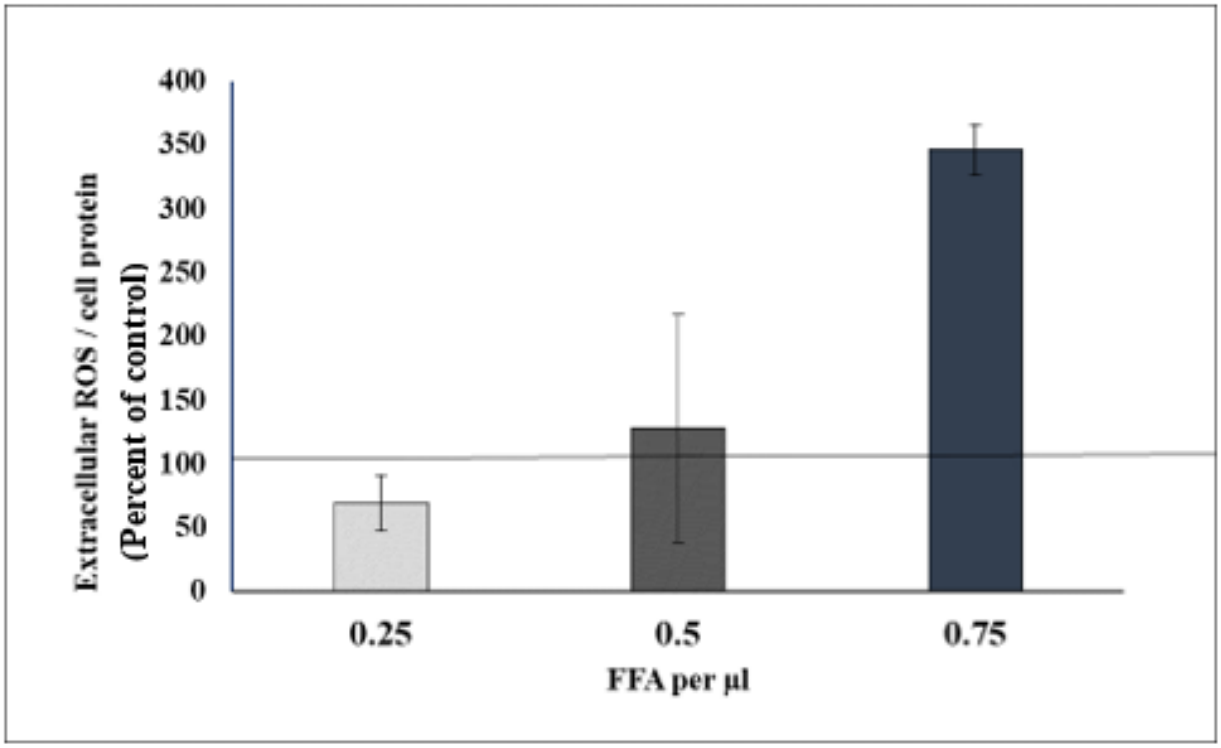

Figure 3.9: Extracellular ROS potentially decreased for 0.25 nmol/µL FFA concentration but increased with 0.5 and 0.75 nmol/µL FFA concentration liberated by CM HPs by LPL vs control

THP-1 cells were incubated with 0.25, 0.5 and 0.75 nmol/µL FFA mixture generated from CM HPs by LPL for 24 hours at 37 °C. All data are normalized with its protein concentration and presented as a percent of control with mean ± SD from duplicate experiments.

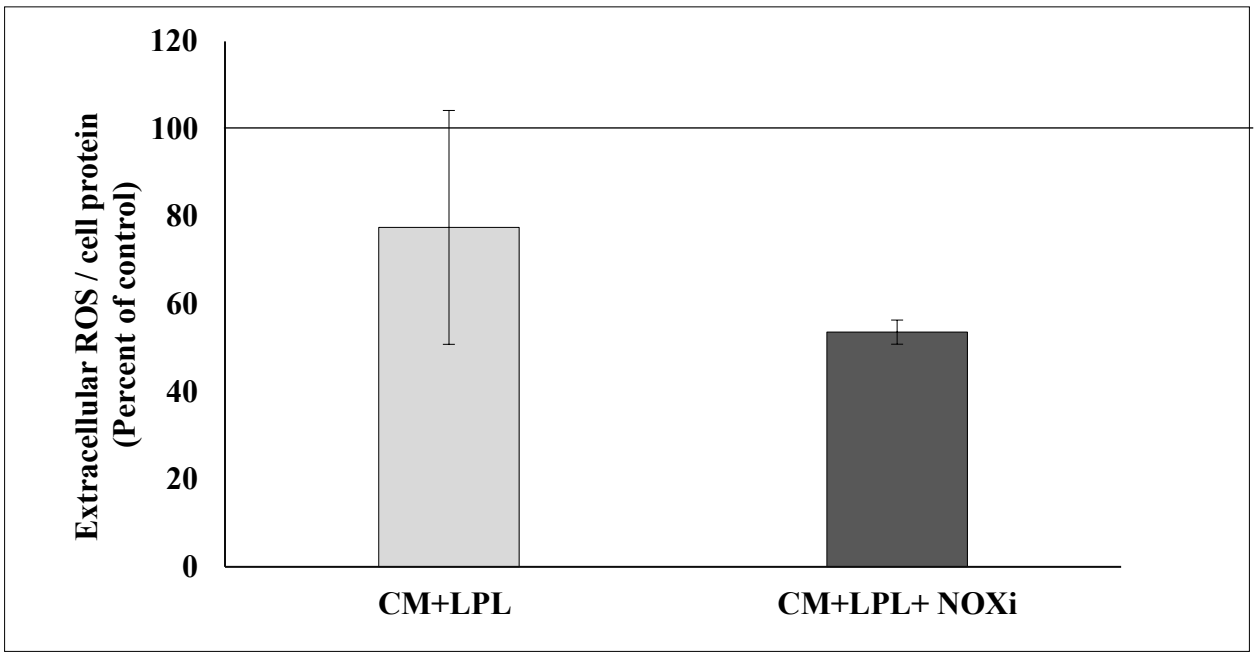

Figure 3.10: Extracellular ROS potentially decreased with CM HPs by LPL with and without NOXi treatment vs control

The THP-1 cells were incubated with 0.5 nmol/µL FFA from HPs of CM and LPL with or without 100 µM NOXi for 24 hours at 37 °C. All data are normalized with its protein concentration and presented as a percent of control with mean ± SD from duplicate experiments (n=2).

3.3. The effect of lipoprotein HPs by LPL with or without NOXi on the MDA production of THP-1 cells and media

ROS are known to cause oxidative degradation of lipids, forming highly reactive and unstable lipid peroxides and, thus, develop atherosclerotic lesions [54]. The decomposition of lipid peroxides results in the formation of TBARS including MDA, hence in this study, we measured TBARS levels for determining the relative lipid peroxide content in THP-1 cells treated with VLDL and CM HPs by LPL, with or without 100 μM NOXi. The lipid peroxidation assay was carried out to measure the resultant intracellular and extracellular MDA from the THP-1 cells after a 24-hour treatment with Lp HPs generated by LPL (as per *section 2.6.2*). The MDA formation due to Lp HPs was compared as a percent of the control. Therefore, MDA formed in the cells or media below 100% indicated lower MDA production in the sample compared to control and vice versa. When the THP-1 macrophages were incubated with 0.5 nmol/μL FFA of VLDL HPs with and without 100 μM NOXi, a potential no change in intracellular MDA of 85.7 ± 13.3 % and 78 ± 15.4 % respectively, was found in relative to control (Figure 3.11). Correspondingly, when the THP-1 cells were incubated with 0.5 nmol/μL FFA of CM with and without 100 μM NOXi, exhibited potential no change in intracellular MDA of 72.9 ± 0.07 % and 91.02 ± 0.41 %, respectively – relative to the control (Figure 3.12). Thus, there was potentially no change in intracellular MDA for both Lps hydrolysis by LPL with and without NOXi treatment in comparison to control.

However, when THP-1 cells were incubated with 0.5 nmol/μL FFA of VLDL HPs, the extracellular MDA was 101.6 ± 1.87 %, and with 100 μM NOXi, the extracellular MDA potentially decreased to 84.8%, ± 4.14 % – all relative to the control (Figure 3.13). Moreover,

`

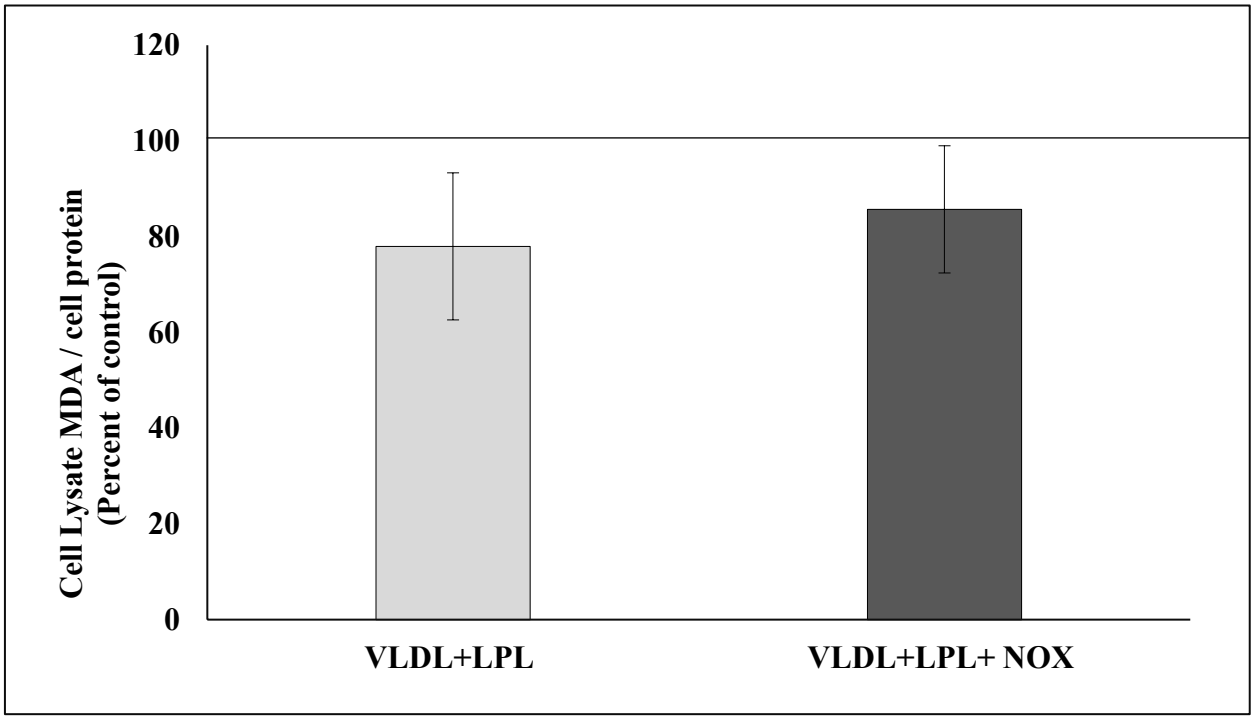

Figure 3.11: Intracellular MDA exhibiting potentially no change with VLDL hydrolysis by LPL with and without NOXi treatment vs control

THP-1 cells were incubated with 0.5 nmol/µL FFA HPs from CM hydrolysis by LPL, with or without 100 µM NOXi, for 24 hours at 37 °C. All data are normalized with its protein concentration and presented as a percent of control with mean ± SD from duplicate experiments (n=2).

`

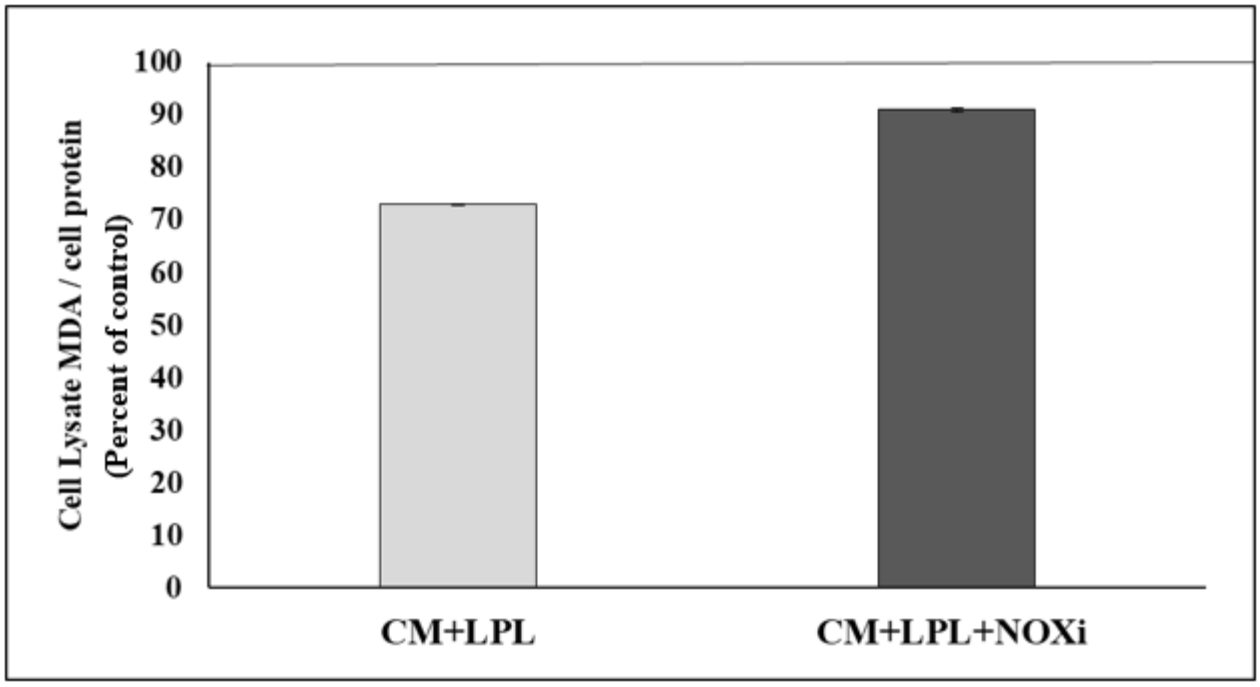

Figure 3.12: Intracellular MDA exhibiting potentially no change with CM hydrolysis by LPL with and without NOXi treatment vs control

THP-1 cells were incubated with 0.5 nmol/µL FFA HPs from CM hydrolysis by LPL, with or without 100 µM NOXi for 24 hours, at 37 °C. All data are normalized with its protein concentration and presented as a percent of control with mean ± SD from duplicate experiments (n=2).

`

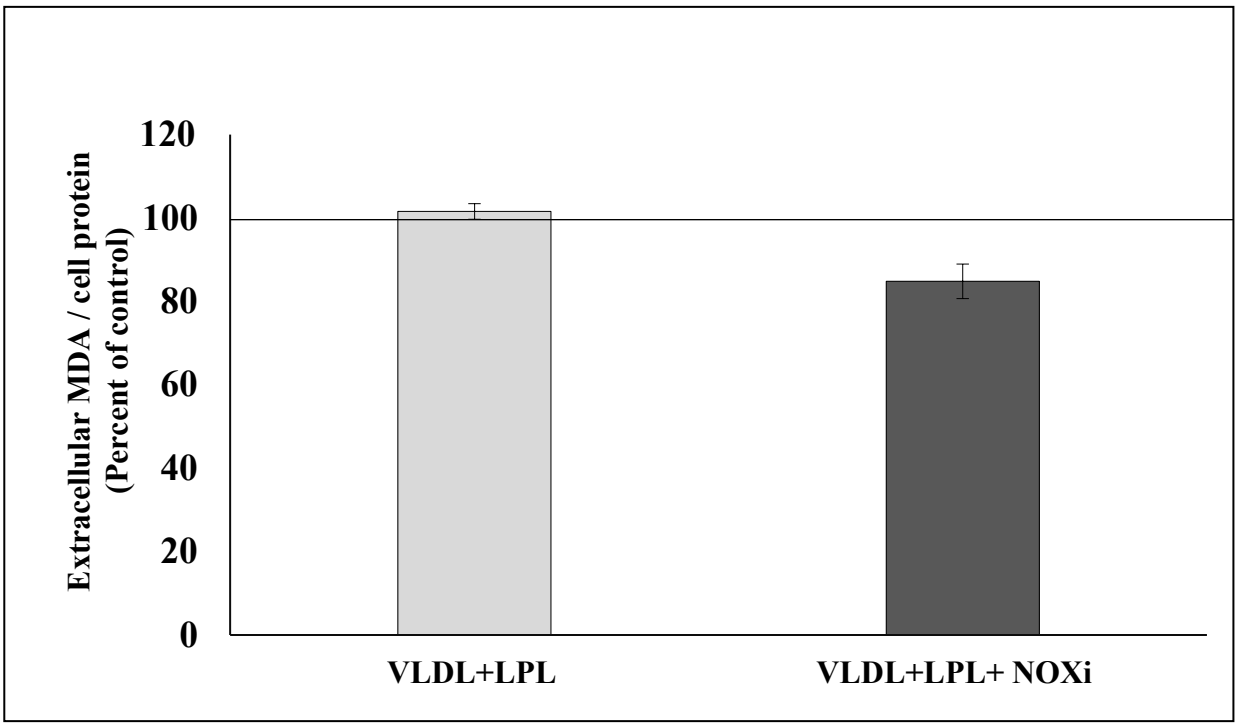

Figure 3.13: Extracellular MDA increased with VLDL hydrolysis by LPL and decreasedwith NOXi treatment vs control

THP-1 cells were incubated with 0.5 nmol/µL FFA HPs generated from VLDL hydrolysis byLPL, without or without 100 µM NOXi for 24 hours at 37 °C. All data are normalized with its protein concentration and presented as a percent of control with mean ± SD from duplicate experiments (n=2).

`

the THP-1cells were incubated with 0.5 nmol/µL FFA of CM HPs, the extracellular MDA was 113.8 ± 19.9 %, whereas with 100 µm NOXi, the extracellular MDA was 94.5 % ± 9.61 %, relative to the control (Figure 3.14).

`

`

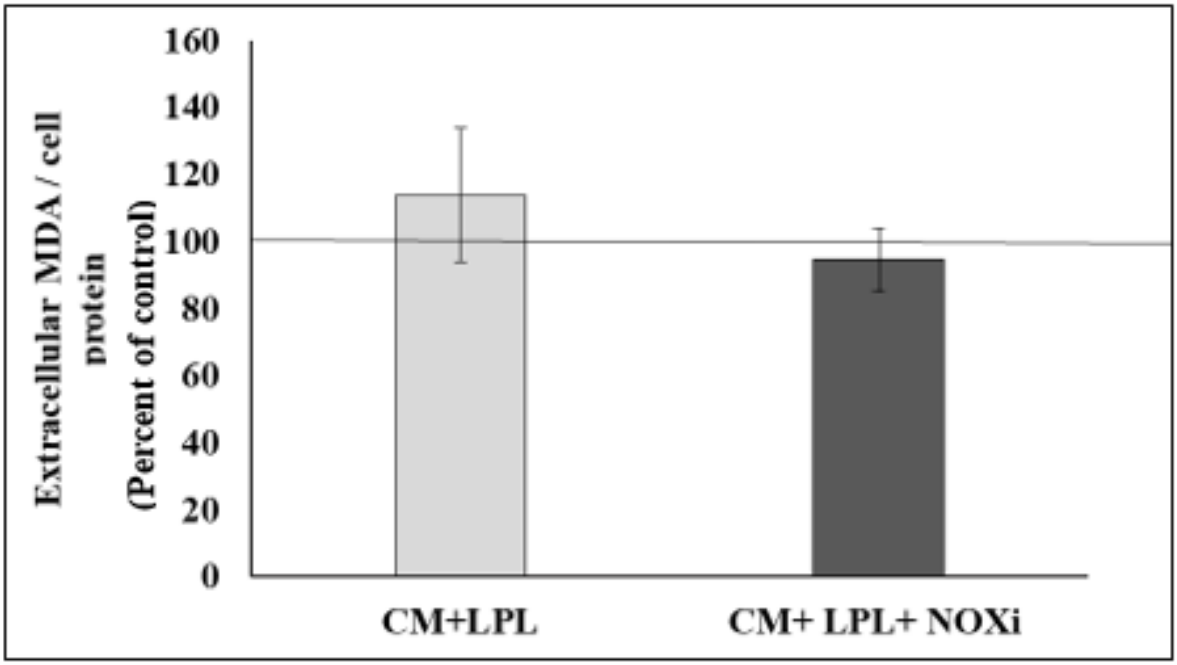

Figure 3.14: Extracellular MDA potentially increased with CM hydrolysis by LPL but decreases with NOXi treatment vs control

THP-1 cells were incubated with 0.5 nmol/µL FFA from HPs of CM and LPL with or without 100 µM NOXi for 24 hours at 37 °C. All data are normalized with its protein concentration and presented as a percent of control with mean ± SD from duplicate experiments (n=2).

3.4. *In silico* analysis of available transcriptomic datasets for Lp lipolysis by LPL in macrophages and astrocytes

In this study, I conducted DEGs analysis using bioinformatics to determine the common genes between macrophage and astrocyte when they are treated with Lp HPs generated by LPL or non-HPs control. The cell lines were selected based on macrophages being linked with CVDs and astrocytes being associated with ischemic stroke [97], as atherosclerosis is the root cause in both the diseases [4]. Moreover, astrocytes play essential roles in neuroinflammation and lipid deposition and the cumulative evidence suggests that astrocyte activation is linked to intracellular brain lipid accumulation [98] and ischemic stroke [97]. Therefore, I investigated if any correlation between genes expression and Lp HPs by LPL in both the cell lines. The available transcriptomic datasets - gene expression analysis of human macrophages exposed to LPL HPs (GSE84791) and expression data from TG lipolysis products treated human astrocytes (GSE76696) - were obtained from the GEO database. The analysis and visualization were carried out using Transcriptome Analysis Console (TAC) 4.0 Software and is illustrated at Figure 3.15. There was a total of 635 DEGs in both cell lines, where 138 DEGs (subsection A in Venn diagram) reported for only astrocytes treated with TG lipolysis vs only TG treatment, and 487 DEGs (subsection B in Venn diagram) for only macrophages treated with LPL HPs vs non-HPs. In addition, we identified 10 DEGs, *ATF3, CHAC1, HMOX1, FAM49A, PSPH, DUSP2, CH25H, IL6, IFI44L,* and *CCNE2* in both the cell lines (subsection C in Venn diagram). The function and foldchanges of the 10 DEGs in both cell lines are shown in Table 2.

`

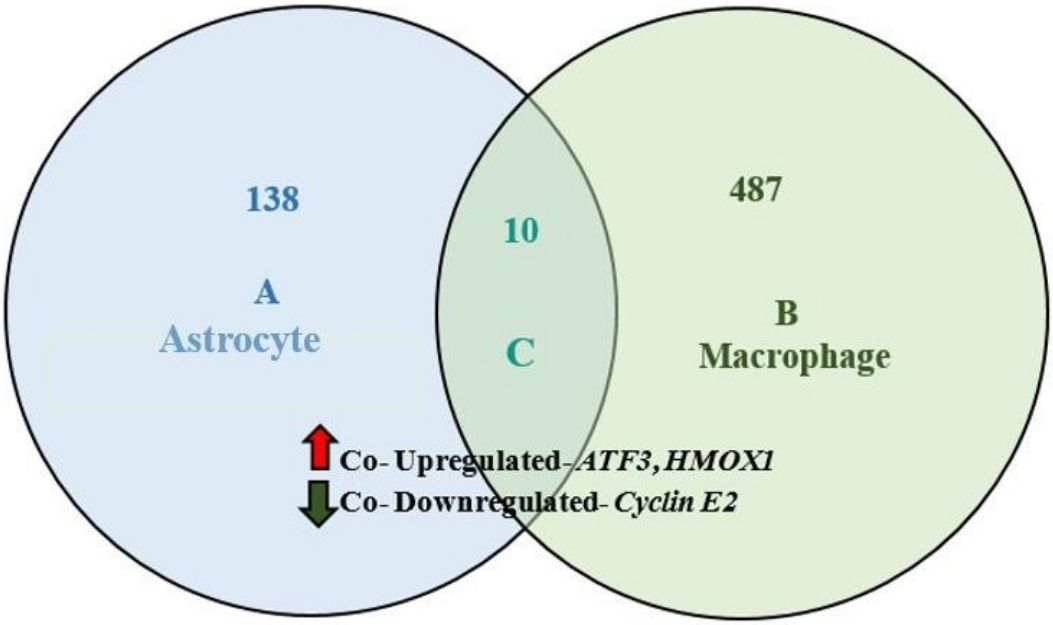

Figure 3.15: Analysis of DEG expression in Macrophage and Astrocyte

Gene expression data from macrophage (GSE84791) and astrocyte (GSE76696) lines were obtained from the GEO database. Among ten common genes, *ATF3* and *HMOX1* were co-upregulated and *CCNE2* was co-downregulated in both the cell lines. The gene expression data were analyzed, and the Venn diagram was generated using TAC 4.0 Software. A= DEG in astrocyte, B= DEG in macrophage, C= common DEG in both cell lines.

`

Table 2: The common genes between macrophages and astrocytes that were affected dueto Lp HP by LPL, where LPL- LPL Hp ; NH- Non- HP

Gene Symbol	Description	Function	Macrophage (LPL Vs, NH)	Astrocyte (LPL Vs, NH)	P-Value
			Fold Change	Fold Change	
CHAC1	ChaC glutathione-specific gamma-glutamylcyclo transferase-1	an ER stress-inducible gene that has a function in the degradation of glutathione [99]	-5.53	6.71	1.54E-05
ATF3	Activating transcription factor 3	a stress-induced transcription factor that plays vital roles in modulating metabolism, immunity, and oncogenesis [100]	2.93	5.21	4.53E-06
HMOX1	Heme oxygenase 1	induced in response to oxidative stressors [101]	2.16	4.21	4.69E-05
FAM49A	Family with sequence Similarity 49, member A phosphoserin e phosphatase 2	Involved in regulation of T cell differentiation and thymus development [102]	-2.06	2.82	0.001
PSPH	Phosphoserine Phosphatase	It catalyzes magnesium-dependent hydrolysis of L-phosphoserine and is involved in an exchange reaction	-2.11	2.53	4.63E-05

`

		between L- serine and L-phosphoserine. [103]			
DUSP2	Dual specificity phosphatase 2	They negatively regulate members of the mitogen-activated protein (MAP) kinase superfamily (MAPK/ERK, SAPK/JNK, p38), which are associated with cellular proliferation and differentiation [104]	-2.29	2.3	8.72E-05
CH25H	Cholesterol 25-hydroxylase	Catalyzes the formation of 25-hydroxycholesterol from cholesterol, leading to repressed cholesterol biosynthetic enzymes [105]	-2.8	2.27	9.70E-07
IL6	Interleukin 6	a soluble mediator with apleiotropic effect on inflammation, immune response, and hematopoiesis [106]	-3.01	2.26	9.68E-06
IFI44L	Interferon-inducedprotein 44	a type I interferon stimulated gen that encodes a protein that has modest activity against hepatitis C virus [107]	-11.24	2.16	3.39E-06

CCNE2	Cyclin E2	Vital for the regulation ofthe cell cycle[108]	-2.54	-2.2	1.54E-05

Note: Analysis type: Expression (Gene); Summarization method: Gene level- Robust Microarray Analysis; Gene-level fold change <-2 or >2; Gene-level –value <0.05; Anova method: Ebayes.

Among these DEGs, *ATF3* and *HMOX1* genes were upregulated, and *CCNE2* was downregulated in both the cell lines (Figure 3.15). Both *ATF3* and *HMOX1* encode stress-induced transcription factors, where ATF3 has been reported to be upregulated due to the ER stress/unfolded protein response [109]. Moreover, a recent study showed *ATF3* may regulate macrophage foam cell formation, as deletion of *ATF3* in *Apoe*$^{-/-}$ mice led to *in vivo* increases in foam cell formation and atherosclerosis progression [110]. *HMOX1* encodes for a stress-induced enzyme that catalyzes the degradation of heme into iron, biliverdin and carbon monoxide. Expression of *HMOX1* and the gene product has been observed during CVD, including ischemic injury. Finally, *CCNE2,* cyclin E2, is a protein coding gene which is vital for the regulation of the cell cycle and downregulation of *CCNE2* is involved with cell cycle arrest and apoptosis. Hence, the results of our *in silico* analysis suggests that Lp HPs generated by LPLinduce both stress and apoptosis in both the cell lines. This now paves a pathway for investigation of endoplasmic ER stress and apoptosis in THP-1 macrophages treated with Lp HPs by LPL vs non-HPs by control, as ER stress is a likely factor that promotes advanced lesional macrophage death.

`

Chapter 4: Discussion

4.1. Lp hydrolysis by LPL modulates NOX expression that may affect the ROS generation in human macrophages

The transition of macrophages to lipid-laden foam cells plays a key role in the development of atherosclerosis [111]. Extensive research shows that macrophage LPL promotes foam cell formation and accelerates atherosclerosis, [112]. Aforementioned, macrophage LPL has been reported to have a pro-atherogenic effect due to its contribution to increased intracellular accumulation of TG and cholesteryl ester, and decreased cholesterol efflux resulting in foam cell formation [113]. Moreover, macrophage NOX is an important source of ROS, where evidence of elevated ROS amplifying the foam cell formation is an integral component in the pathogenesis of atherosclerosis [114]. In this study, I analyzed changes in ROS in THP-1 macrophages cell lysate and media when treated with HPs of VLDL and CM generated by LPL for 24 hours. For the Lp hydrolysis by LPL, the FFA generated was diluted to 0.25, 0.5, and 0.75 nmol/µl, which falls under the human normal physiological concentration range [115]. Furthermore, I assessed if HPs of Lp by LPL may have induced NOX-mediated ROS and whether NOXi may reduce intracellular and extracellular ROS in THP-1 macrophages.

Previously, study with FFA from VLDL lipolysis by LPL were shown to enhance ROS production in HAEC [96]. The mechanism of FFA inducing ROS has been reported, such that the polyunsaturated fatty acid (PUFA) can stimulate ROS production by NOX located in the membrane of macrophages [116]. In neutrophils, the NOX enzyme complexes are composed of the heterodimer catalytic core formed by the two membrane subunits (p47-phox and p22-phox). There are four regulatory cytosolic components (p67-phox, p40-phox, gp91-phox, and Rac) required for NOX enzyme activation via phosphorylation of the Ser or Thr residue of p47-phox subunit [117]. This suggests that PUFA stimulate a conformational change of p47-phox to a state

capable of interacting with p22-phox, an event proportional to superoxide production [119]. Additionally, amphipathic property of PUFA facilitates the production of elevated ROS via NOX [116]. As the amphipathic property of PUFA causes affinity towards NOX components including, Rac GTPs, cytochrome b558 and cytochrome C [119,120], their interaction causes changes to the conformation of NOX components. These changes enhance the complex's affinity towards oxygen, and thereby generating ROS [116]. Hence, ROS is produced due to confirmational changes of NOX because of interactions with PUFA.

I expected enhanced intracellular and extracellular ROS levels with an increasing concentration of FFA from the lipolysis of Lp by LPL in THP-1 macrophages. Interestingly, the 0.25 and 0.5 nmol/µL FFA concentrations of HPs from both VLDL and CM Lps by LPL accounted for lower intracellular ROS in comparison to control, and the 0.25 nmol/µL FFA concentration resulted in lower extracellular ROS in comparison to control. The decrease in ROS in the treated cells, relative to the controls, may be due to activation of the phosphoinositide 3-kinase (PI3K)/ protein kinase B (Akt) pathway. The activated Akt signaling pathway could induce nuclear translocation of nuclear factor-erythroid factor 2-related factor 2 (Nrf2), a basic leucine zipper region transcription factor of the Cap n'Collar family, which is bound to the E3 ubiquitin ligase Keap1 in the cytosol [121]. The transcription factor Nrf2 is predominantly activated in response to oxidative stress. Following activation, Nrf2 translocates to the nucleus and binds to the antioxidant response element (ARE) or the electrophile-response element in the promoter region of Nrf2 target genes. This binding results in the coordinated expression and activation of antioxidant, antiapoptotic, metabolic, and detoxification proteins. Proteins with antioxidant activity regulated by Nrf2 include SOD, catalase, HMOX-1, glutathione peroxidase 1 and NADPH: quinone oxidoreductase 1 [122]. As oxidative stress occurs due to an imbalance of the pro-oxidant and antioxidant system, the level of ROS was lowered as the antioxidant system was

`

increased to counteract the oxidative stress. Hence, the ROS was maybe potentially lowered due to the activation of the antioxidant system of the cells which successfully lowered the potential overall ROS. The above suggests that the 0.25 and 0.5 nmol/µL FFA concentrations may have stimulated macrophage intracellular antioxidant defense systems that reduces the harmful effects of ROS.

On the other hand, 0.75 nmol/µL FFA produced potentially very high ROS levels, which may be due to high ROS, that could have overwhelmed the antioxidant system of the macrophage. Overall, these data suggest that LPL has a protective function within THP-1 macrophages with lower FFA concentration (0.25 and 0.5 nmol/µl) whereas, with higher FFA concentration (0.75 nmol/µl) of Lp lipolysis product by LPL, tends to cause overproduction of ROS.

The resultant ROS level in the media was higher when compared to the cell lysate for the 0.25 and 0.5 nmol/µL FFA concentrations. NOX has been known to be the main source of ROS delivery to the extracellular space during respiratory bursts and phagocytosis [123]. The major intracellular ROS production sites exist within mitochondria, including the NOX present in mitochondria, Complex 1, Complex 2, and Complex 3 of electron transport chain [124], mitochondrial alpha-glycerophosphate dehydrogenase [125] and alpha-ketoglutarate dehydrogenase [126]. Additionally, the ER accounts for ROS formation during the metabolic transformation of PUFA [127]. Hence, higher ROS in media could be due to higher NOX activity in the macrophage membrane versus other sources of intracellular ROS. Moreover, intracellular ROS may be formed rapidly, and a 24-hour treatment maybe too long to detect theformation. To confirm this, intracellular and extracellular ROS readings could be taken every hour during a 24-hour treatment. In future studies, assessment of ROS production in mitochondria and ER of THP-1 macrophage when incubated with Lp HPs by LPL may provide more detailed insights about

`

intracellular ROS in foam cells. Although, for 0.75 nmol/μL FFA concentration, the ROS level in cell lysate was higher than in media, which could be due to the higher and longer activity of NOX.

Akt is a well-established master kinase involved in various biological processes, including cell growth and proliferation, apoptosis, and angiogenesis [128]. Akt activation occurs when PI3K is activated due to the binding of growth factors to a G protein-coupled receptor or receptor tyrosine kinase, including platelet-derived growth factor receptor or epidermal growth factor receptor [129]. Previously, a study reported that the FFA component of the total Lp HPs by LPL, predominantly palmitoleate, phosphorylates Ser-473 in the regulatory region and Thr-308 in the active site and activate Akt in a dose-dependent manner in THP-1 macrophages [130]. The relevance of PI3K/Akt signaling in activating the NOX enzyme has been confirmed, as suppression of NOX activity was observed due to PI3K inhibitor wortmannin or *Akt1* knockout [131]. Therefore, activation of Akt may play a role in the NOX-induced ROS generation in THP-1 macrophages when incubated with Lp HPs by LPL.

The cells associated with atherosclerosis progression, including VSMCs, ECs, and macrophages, have been reported to have dysregulation of the PI3K/Akt signaling pathway [132]. The expression and activation of Akt isoforms: Akt1, Akt2, and Akt3 are different in macrophages than in VSMCs and ECs. Akt1 is predominantly expressed in both VSMCs andEC, whereas Akt1 and Akt2 are both highly expressed to same levels in macrophages [133- 135]. Regulation of survival, cytokine secretion, NO synthesis, and programming in macrophages are carried out by the Akt pathway [136]. In atherosclerosis, Akt isoforms in macrophages may have entirely distinct or even contradictory effects [137]. Studies report that macrophage Akt1 and Akt2 exhibit opposing outcomes for M1/M2 polarization,

`

cholesterol accumulation, and inflammation. Akt2 is atherogenic because it stimulates inflammation, foam cell formation, M1 phenotype, and chemokine receptor type2-mediated migration. On the other hand, studies reported Akt3 to impede macrophage foam cell formation and thus function as athero-protective [138]. Thus, in macrophages, Akt1 and Akt3 are protective against atherosclerosis although, Akt3 promotes atherosclerosis.

Interestingly, studies have shown that low concentrations of NOX-mediated H_2O_2 can activate the PI3K/Akt pathway, which results in increased cell proliferation [139]. It has been proposed that a small increase of H_2O_2 via NOX1 causes enhanced cell cycle progression, although prolonged high levels of H_2O_2 lead to cell arrest and subsequent apoptosis following sustained arrest [140]. This suggests that the HPs generated by LPL in THP-1 macrophages may induce NOX-mediated ROS due to activation of PI3K/Akt signaling, where NOX-generated ROS may sustain PI3K/Akt signaling to result in overproduction of ROS. The overproduction ofROS upregulates the snoRNA as previously shown by Holley *et al.* [95], where the siRNA-mediated knockdown of NOX decreased both snoRNA and ROS. Hence, elevated snoRNA in macrophages increases oxidative stress and may lead to foam cell formation (Figure 4.1). The model shows that the HPs generated by LPL may stimulate NOX-mediated ROS production in THP-1 macrophages because of PI3K/Akt signaling activation, where the activation is sustained due to the NOX-generated ROS generating enhanced ROS. The enhanced ROS further may upregulate the snoRNA expression in the macrophages for them to convert to foam cells.

`

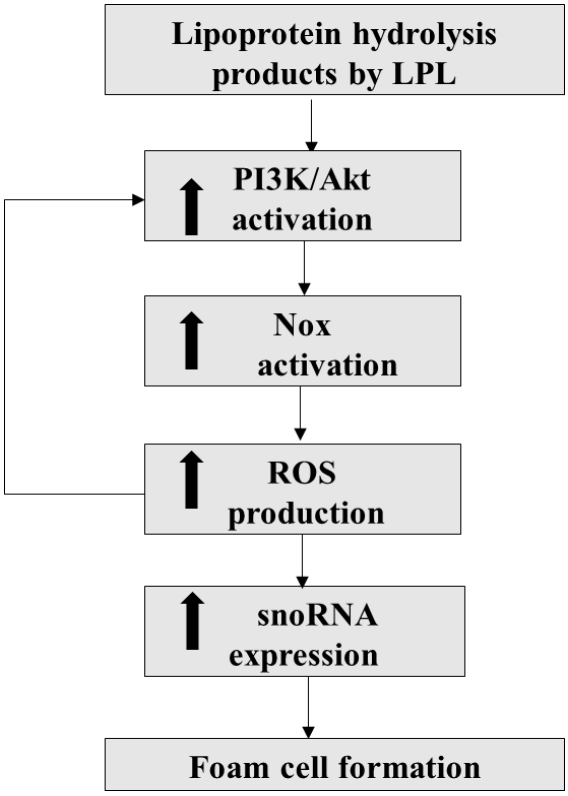

Figure 4.1: Proposed mechanism in THP-1 cells to convert to foam cells

The LPL HPs have been shown to significantly increase PI3K/Akt activation in macrophages. The PI3K/Akt signaling stimulates NOX-mediated-ROS generation, which further sustains activation of PI3K/Akt signaling, leading to ROS overproduction. The enhanced ROS may upregulate the snoRNA expression in the THP-1 macrophage to promote foam cell formation.

`

For the inhibitory study of ROS production, the NOXi apocynin was used. Apocynin was chosen because it is one of the most extensively studied NOXi [141]. Moreover, Rutledge *et al*. [96] showed that FFA-mediated increases of ROS in HAEC was inhibited by using 100 μM apocynin. For our inhibitory study, a 0.5 nmol/μL FFA concentration of Lp hydrolysis by LPL was chosen for treating the THP-1 macrophages, as 0.5 nmol/μL FFA falls in the mid-range of the select concentration of this study. As 0.5 nmol/μL FFA concentration of VLDL HPs by LPL played a protective role in lowering intracellular ROS, NOXi lowered it further relative to control. Intracellular ROS generated by CM hydrolysis by LPL was higher, and the addition of NOXi lowered the ROS, as anticipated. The ability of NOXi to lower ROS was mirrored in extracellular ROS production in THP-1 cell media in response to CM HPs by LPL in comparison to control. On the other hand, the extracellular ROS was pronounced when VLDL HPs by LPL were treated with or without NOXi compared to control, although with NOXi there was slight decrease in ROS compared to without NOXi. Even though apocynin is known as a direct ROS scavenger, other studies had suggested apocynin to have paradoxical effect, being a pro-oxidant stimulating ROS production depending on its concentration.

In summary, for treatment of VLDL HPs by LPL in THP-1 macrophages, there was no effect of NOXi observed, as the intracellular ROS was lower than control and extracellular ROS was higher than control, with or without NOXi. Conversely, for CM HPs by LPL, there was a NOXi inhibitory effect, as the enhanced intracellular ROS without NOXi was decreased with NOXi in comparison to control. However, there was no effect of NOXi observed as the extracellular ROS was lower than control with or without NOXi.

`

4.2. Modulation of NOX expression due to Lp hydrolysis by LPL product does not affect the extracellular MDA production in human macrophages

A plethora of evidence has documented the ability of ROS to attack membrane lipids containing carbon-carbon double bonds (such as PUFA chains within PL) and damage them via lipid peroxidation. The lipid peroxidation of FFA can arise from both enzymatic and non-enzymatic mechanisms. In enzymatic peroxidation, lipoxygenase plays a role in the generation of lipid peroxides. On the other hand, in a non-enzymatic mechanism, NOX-induced ROS can remove hydrogen from a CH_2 group of PUFAs, following the production of lipid-hydroperoxide molecules (LOOH) and new dienyl radicals, which allows the lipid peroxidation chain reaction to move forward. The generated LOOHs are then subjected to degradation with the formation of TBARS including MDA, a reactive aldehyde. The MDA can furthermore propagate oxidative damage and thus act as downstream mediators of oxidative stress. Increased lipid peroxidation disrupts the integrity of different cellular structures including DNA and proteins [142]. Moreover, the lipid peroxidation-mediated products can interact with membrane receptors and transcription factors to stimulate signaling for apoptosis. Activation of both the intrinsic and extrinsic apoptotic signaling pathways leading to cellular death occurs due to an increase in MDA [143,144]. Thus, enhanced ROS may increase lipid peroxidation,altering structures of cellular macromolecules, and resulting in cell death.

In atherogenesis, enhanced lipid peroxidation is reported to be involved during the conversion of macrophages into foam cells, as it promotes LDL oxidation and accelerates arterial macrophages to take up ox-LDL [145]. Therefore, in this study, we quantified the TBARS levels for determining the relative lipid peroxide with or without NOXi in THP-1 cells and media when treated with VLDL and CM HPs by LPL for 24 hours. I used 0.5

`

nmol/μL FFA from VLDL and CM HPs by LPL, and HPs from both the Lps resulted in lower intracellular MDA levels, relative to the control – with or without NOXi. As the cellular ROS level with and without NOXi was lower compared to control, the cellular MDA level showed the same effect. Here, the effect of NOXi cannot be deduced as the level of MDA without NOXi was already low.

However, the treatment with 0.5 nmol/μL FFA from VLDL HPs by LPL induced similar extracellular MDA level relative to control without NOXi, which decreased with NOXi. On the other hand, the treatment with 0.5 nmol/μL FFA from CM HPs by LPL induced similar extracellular MDA level relative to control with or without NOXi. This suggests that FFA from both Lps generated by LPL did not impact on the extracellular MDA.

4.3. Lipoprotein HPs induces stress-induced genes and causes cell cycle arrest in macrophages and astrocytes

To attempt to explain how Lp HPs by LPL may alter the common gene expression in macrophages and astrocytes, as both the cells play a central role in atherosclerosis, I investigated the common DEGs in response to Lp HPs by LPL. The results showed that there were a total 10 common genes, of which *CHAC1, FAM49A, PSPH, DUSP2, CH25H, IL6, and IFI44L* showed a different trend in regulation, and *ATF3 and HMOX1* were upregulated and *Cyclin E2* was downregulated in both cell lines (the fold changes of the 10 DEGs in two cell lines are shown in Table 2).

Lp lipolysis products by LPL in both cell lines resulted in the upregulation of *ATF3*, which is known to be involved in the intricate process of the cellular stress response and is thought to play an important role in the cardiovascular system [137]. Studies have shown that myocardial ischemia to activate unfolded protein response (UPR) and ATF3 via ER stress [146]. Furthermore, ATF3 has been observed to negatively regulate pro-inflammatory cytokine expression in macrophages that are known to accelerate atherosclerosis [147]. On the other hand, in astrocytes, it has been observed that the ATF3 expression was upregulated at the transcriptional level by Nrf2 [148]. As previously mentioned, Nrf2 binds to the ARE in promoters in response to ROS and enhances the antioxidant enzymes of the cells [149]. Kim *et al.*, showed that ATF3 expression in astrocytes was diminished in Nrf2-depleted cells [148], indicating Nrf2 involved in upregulation of ATF3. Thus, in my study, upregulation of ATF3 in both cell lines due to Lp hydrolysis products by LPL suggests ROS to play role in Nrf2 and UPR/ER stress activation. More studies need to be done to confirm this.

`

Additionally, *HMOX1*, a key player in the maintenance of an antioxidant/oxidant homeostasis in the body, showed increased expression in both cell lines due to Lp HPs by LPL. A large body of evidence shows that *HMOX1* is highly upregulated due to ox-LDLs in atherosclerotic lesions, including macrophages, foam cells and ECs [150]. Moreover, there was evidence of an increase in *HMOX1*, reflecting an adaptive response to compensate for oxidative stress. In macrophages, *HMOX1* was reported to provide antioxidant and anti-inflammatory effects as diminished *HMOX1* expression in peritoneal macrophages caused enhanced ROS formation and increased inflammatory cytokines [151-154]. Furthermore, upregulation of *HMOX1* expression accounts for the decrease in lipid loading and foam cell formation [153], and it has been shown to play a role in macrophage differentiation and polarization. ROS is a known activator of Nrf2 pathway [154], and Swindell *et al.* suggested that up-regulation of *HMOX1* in astrocytes may be due to an Nrf2-mediated mechanism [155]. My results suggest that both *ATF3* and *HMOX1* might be activating Nrf-2due to ROS generation and thus, the role of LPL needs to be confirmed.

Finally, the downregulation of *CCNE2* due to Lp HPs in both macrophage and astrocyte cell lines suggests there is halting of the cell cycle, as the expression of cyclin E is a crucial factor accelerating cell entry into the S-phase and cell proliferation [156]. This indicates that LPL plays a role in slowing down the cell cycle, and the progression of atherosclerosis in both macrophages and astrocytes. Thus, macrophages treated with Lp HPs should be assessed for ER stress and apoptosis, based on my bioinformatic analysis.

`

4.4. Study limitations

In this study, only two sets of experiments were performed to assess resultant ROS and MDA levels in THP-1 cells when treated with Lp HPs by LPL, with and without NOXi. I was not able to complete the third set of experiment due to many interruptions in the research work, which includes two COVID-19 lockdowns and a relocation of the research laboratory.

Furthermore, in the ROS and MDA study, selecting 0.5 nmol/µL FFA concentration of HPs was a limitation. The 0.5 nmol/µL FFA concentration of HPs by LPL induced lower ROS and MDA than the control, hence the inhibitory effect of NOXi could not be validated. I chose this concentration because 0.5 nmol/µL FFA is the middle concentration from the select concentration of Lp HPs by LPL in the study. As I had a time limitation with the lockdowns, I had to carry out the non-inhibitory and inhibitory of NOXi analysis side by side, and I later came to conclusion that 0.75 nmol/µL FFA concentration of HPs would have been the better choice.

Moreover, another limitation to the study is the use of PBS to dilute the Lps instead of using RPMI medium, as this may have caused nutrient deprivation in the cells.

4.5. Future directions

The present study suggests NOX could be a potential target to investigate in future studies. My data indicate that 0.75 nmol/µL or higher FFA concentration generated from both Lps by LPL could be assessed in the THP-1 cell system for ROS and MDA levels. Furthermore, selective inhibitors for NOX, such as the NOX1/4 inhibitor GKT136901, could be used. Additionally, the ROS and MDA measurements can be taken every hour to elucidate the effect of Lp hydrolysis product by LPL, as 24 hours was a long treatment time. Finally, my bioinformatics study indicates an upregulation of stress-inducing genes and downregulation of a gene involved in the cell cycle in macrophage and astrocyte cell lines when subjected to Lp hydrolysis by LPL. Thus, the Nrf2 pathway, ER stress, and apoptosis could be investigated in macrophages to determine the effect

of LPL.

4.6.Overall conclusion

This study has shown that LPL HPs may promote the conversion of macrophages into foam cells through the overproduction of NOX-mediated ROS. The increase of ROS may be through activation of PI3K/Akt signaling and may have resulted in upregulation of snoRNA expression previously identified by our laboratory in a THP-1 model of atherosclerosis Another finding of this study is that the lipolysis of Lp by LPL does not change in intracellular lipid peroxide level via NOX pathway in THP-1 macrophages, although extracellular MDA was decreased with NOXi. Furthermore, the *in silico* study using macrophage and astrocyte cell lines determined there was an upregulation of stress-inducing genes and downregulation of agene involved in the cell cycle, that may have led to the cell death pathway in both cell lines [156]. Overall, the results of this study highlight the potential central role of LPL HPs in the conversion of foam cells and atherosclerosis progression.

`

5. References

[1] World Health Organization. Cardiovascular diseases (CVDs) Fact Sheet. 2021. Available online: https://www.who.int/news-room/fact-sheets/detail/cardiovascular-diseases-(cvds) (accessed on 24 May 2022).

[2] Moore, K. J., & Tabas, I. (2011). Macrophages in the pathogenesis of atherosclerosis. Cell, 145, 341-355.

[3] Park, I., Kassiteridi, C., & Monaco, C. (2017). Functional diversity of macrophages in vascular biology and disease. Vascular Pharmacology, 99, 13-22.

[4] Lusis, A. J. (2000). Atherosclerosis. Nature, 407, 233-241.

[5] Gimbrone Jr, M. A. (1999). Vascular endothelium, hemodynamic forces, and atherogenesis. The American Journal of Pathology, 155, 1-5.

[6] Borén, J., Olin, K., Lee, I., Chait, A., Wight, T. N., & Innerarity, T. L. (1998). Identification of the principal proteoglycan-binding site in LDL. A single-point mutation in apo-B100 severely affects proteoglycan interaction without affecting LDL receptor binding. The Journal of Clinical Investigation, 101, 2658-2664.

[7] Goldstein, J. L., Ho, Y. K., Basu, S. K., & Brown, M. S. (1979). Binding site on macrophages that mediates uptake and degradation of acetylated low density lipoprotein, producing massive cholesterol deposition. Proceedings of the National Academy of Sciences of the United States of America, 76, 333-337.

[8] Dong, Z. M., Chapman, S. M., Brown, A. A., Frenette, P. S., Hynes, R. O., & Wagner, D. D. (1998). The combined role of P-and E-selectins in atherosclerosis. The Journal of Clinical Investigation, 102, 145-152.

`

[9] Collins, R. G., Velji, R., Guevara, N. V., Hicks, M. J., Chan, L., & Beaudet, A. L. (2000). P-selectin or intercellular adhesion molecule (ICAM)-1 deficiency substantially protects against atherosclerosis in apolipoprotein E–deficient mice. The Journal of Experimental Medicine, 191, 189-194.

[10] Smith, J. D., Trogan, E., Ginsberg, M., Grigaux, C., Tian, J., & Miyata, M. (1995). Decreased atherosclerosis in mice deficient in both macrophage colony-stimulating factor (op) and apolipoprotein E. Proceedings of the National Academy of Sciences of the United States of America, 92, 8264-8268.

[11] Libby, P. (2000). Cholesterol and atherosclerosis. Biochimica et Biophysica Acta – Molecular and Cell Biology of Lipids, 1529, 299-309.

[12] Kunjathoor, V. V., Febbraio, M., Podrez, E. A., Moore, K. J., Andersson, L., Koehn, S Freeman, M. W.,Rhee, J. S.,Silverstein, R., & Hoff, H. F. (2002). Scavenger receptors class AI/II and CD36 are the principal receptors responsible for the uptake of modified low density lipoprotein leading to lipid loadingin macrophages. Journal of Biological Chemistry, 277, 49982-49988.

[13] Tontonoz, P., Nagy, L., Alvarez, J. G., Thomazy, V. A., & Evans, R. M. (1998). PPARγ promotes monocyte/macrophage differentiation and uptake of oxidized LDL. Cell, 93, 241-252.

[14] Schönbeck, U., Sukhova, G. K., Shimizu, K., Mach, F., & Libby, P. (2000). Inhibition of CD40 signaling limits evolution of established atherosclerosis in mice. Proceedings of the National Academy of Sciences of the United States of America, 97, 7458-7463.

[15] Schönbeck, U., Mach, F., Sukhova, G. K., Herman, M., Graber, P., Kehry, M. R., & Libby, P. (2000). CD40 ligation induces tissue factor expression in human vascular smooth muscle cells. The American Journal of Pathology, 156, 7-14.

`

[16] Brody, T. (1999). Classification of biological structure. Nutritional Biochemistry (2nd ed.), Academic Press, 2, 1-56.

[17] Feingold, K. R., & Grunfeld, C. (2012). Lipids: a key player in the battle between the host and microorganisms1. Journal of Lipid Research, 53, 2487-2489.

[18] Feingold, K. R. (2021). Introduction to Lipids and Lipoproteins. In Endotext [Internet]. MDText.com, Inc. Available online: https://www.ncbi.nlm.nih.gov/books/NBK305896/ (accessed on 26 May 2022).

[19] Feldman, M., Friedman, L. S., & Brandt, L. J. (2020). Sleisenger and Fordtran's gastrointestinal and liver disease E-book: pathophysiology, diagnosis, management. Elsevier Health Sciences, 72, 1135-1153

[20] Brown, M. S., & Goldstein, J. L. (1986). A receptor-mediated pathway for cholesterol homeostasis. Science, 232, 34-47.

[21] Herz, J. (1993). The LDL-receptor-related protein-portrait of a multifunctional receptor. Current Opinion in Lipidology, 4, 107-113.

[22] Rigotti, A., Miettinen, H. E., & Krieger, M. (2003). The role of the high-density lipoprotein receptor SR-BI in the lipid metabolism of endocrine and other tissues. Endocrine Reviews, 24, 357-387.

[23] Cooper, A. D. (1997). Hepatic uptake of chylomicron remnants. Journal of Lipid Research, 38, 2173-2192.

[24] Soutar, A. K., Myant, N. B., & Thompson, G. R. (1982). The metabolism of very low density and intermediate density lipoproteins in patients with familial hypercholesterolaemia. Atherosclerosis, 43, 217-231.

`

[25] Zambon, A., Bertocco, S., Vitturi, N., Polentarutti, V., Vianello, D., & Crepaldi, G. (2003). Relevance of hepatic lipase to the metabolism of triacylglycerol-rich lipoproteins. Biochemical Society Transactions, 31, 1070-1074.

[26] Fielding, C. J., & Fielding, P. E. (2008). Dynamics of lipoprotein transport in the circulatory system. In Biochemistry of lipids, lipoproteins and membranes. Elsevier, 5, 533-553.

[27] Lewis, G. F., & Rader, D. J. (2005). New insights into the regulation of HDL metabolism and reverse cholesterol transport. Circulation Research, 96, 1221-1232.

[28] Kunitake, S. T., La Sala, K. J., & Kane, J. P. (1985). Apolipoprotein AI-containing lipoproteins with pre-beta electrophoretic mobility. Journal of Lipid Research, 26, 549-555.

[29] Oram, J. F., Lawn, R. M., Garvin, M. R., & Wade, D. P. (2000). ABCA1 is the cAMP-inducible apolipoprotein receptor that mediates cholesterol secretion from macrophages. Journal of Biological Chemistry, 275, 34508-34511.

[30] Miksztowicz, V., Schreier, L., McCoy, M., Lucero, D., Fassio, E., Billheimer, J, Rader, D.J., & Berg, G. (2014). Role of SN1 lipases on plasma lipids in metabolic syndrome and obesity. Arteriosclerosis, Thrombosis, and Vascular Biology, 34, 669-675.

[31] Hide, W. A., Chan, L., & Li, W. H. (1992). Structure and evolution of the lipase superfamily. Journal of Lipid Research, 33, 167-178.

[32] Goldberg, I. J., Le, N. A., Ginsberg, H. N., Krauss, R. M., & Lindgren, F. T. (1988). Lipoprotein metabolism during acute inhibition of lipoprotein lipase in the cynomolgus monkey. The Journal of Clinical Investigation, 81, 561-568.

[33] Dugi, K. A., Dichek, H. L., & Santamarina-Fojo, S. (1995). Human hepatic and lipoprotein lipase: the loop covering the catalytic site mediates lipase substrate specificity. Journal of

`

Biological Chemistry, 270, 25396-25401.

[34] Merkel, M., Loeffler, B., Kluger, M., Fabig, N., Geppert, G., Pennacchio, L. A, Heeren, J. & Laatsch, A. (2005). Apolipoprotein AV accelerates plasma hydrolysis of triglyceride-rich lipoproteins by interaction with proteoglycan-bound lipoprotein lipase. Journal of Biological Chemistry, 280, 21553-21560.

[35] Olivecrona, G. (2016). Role of lipoprotein lipase in lipid metabolism. Current Opinion in Lipidology, 27, 233-241.

[36] Beigneux, A. P., Davies, B. S., Gin, P., Weinstein, M. M., Farber, E., Qiao, X., Young, S. G., Peale F., Bunting, S., Walzem., R. L., Wong, J. S., Blaner, W. S., Ding, Z., Melford, K., Wongsiriroj, N., Shu, X., Sauvage, F.D, Ryan, R.O, Fong, L.G. & Bensadaoun, A. (2007). Glycosylphosphatidylinositol-anchored high-density lipoprotein-binding protein 1 plays a critical role in the lipolytic processing of chylomicrons. Cell Metabolism, 5,279-291.

[37] Cheng, C. F., Oosta, G. M., Bensadoun, A., & Rosenberg, R. D. (1981). Binding of lipoprotein lipase to endothelial cells in culture. Journal of Biological Chemistry, 256, 12893-12898.

[38] Shimada, K., Gill, P. J., Silbert, J. E., Douglas, W. H., & Fanburg, B. L. (1981). Involvement of cell surface heparin sulfate in the binding of lipoprotein lipase to cultured bovine endothelial cells. The Journal of Clinical Investigation, 68, 995-1002.

[39] Camps, L., Reina, M., Llobera, M., Vilaro, S., & Olivecrona, T. (1990). Lipoprotein lipase: cellular origin and functional distribution. American Journal of Physiology-Cell Physiology, 258, C673-C681.

[40] Camps, L., Reina, M., Llobera, M., Bengtsson-Olivecrona, G., Olivecrona, T., & Vilaro, S.

`

(1991). Lipoprotein lipase in lungs, spleen, and liver: synthesis and distribution. Journal of Lipid Research, 32, 1877-1888.

[41] O'brien, K. D., Gordon, D., Deeb, S., Ferguson, M., & Chait, A. (1992). Lipoprotein lipase is synthesized by macrophage-derived foam cells in human coronary atherosclerotic plaques. The Journal of Clinical Investigation, 89, 1544-1550.

[42] Griffon, N., Budreck, E. C., Long, C. J., Broedl, U. C., Marchadier, D. H., Glick, J. M., & Rader, D. J. (2006). Substrate specificity of lipoprotein lipase and endothelial lipase: studies of lid chimeras. Journal of Lipid Research, 47, 1803-1811.

[43] Cohen, J. C. (2003). Endothelial lipase: direct evidence for a role in HDL metabolism. The Journal of Clinical Investigation, 111, 318-321.

[44] Merkel, M., Eckel, R. H., & Goldberg, I. J. (2002). Lipoprotein lipase. Journal of Lipid Research, 43, 1997-2006.

[45] Braun, J. E., & Severson, D. L. (1992). Regulation of the synthesis, processing and translocation of lipoprotein lipase. Biochemical Journal, 287, 337-347.

[46] Arora, R., Nimonkar, A. V., Baird, D., Wang, C., Chiu, C. H., Horton, P. A., Trauger, J. W., Hanrahan, S., Cubbon, R., Weldon, S., Tschantz, W. R., Mueller, S., Brunner, R., Lehr, P.,Meir, P.,Ottl, J.,Voznesensky, A., Pandey, P., Smith,T.M , Stojanovic, A., Flyer, A., Benson,T.E, & Romanowski, M. J. (2019). Structure of lipoprotein lipase in complex with GPIHBP1. Proceedings of the National Academy of Sciences of the United States of America, 116, 10360-10365.

[47] Hayne, C. K., Yumerefendi, H., Cao, L., Gauer, J. W., Lafferty, M. J., Kuhlman, B., Neher, S. B. & Erie, D. A., (2018). We FRET so you don’t have to: New models of the lipoprotein

`

lipase dimer. Biochemistry, 57, 241-254.

[48] Jansen, H., Verhoeven, A. J., & Sijbrands, E. J. (2002). Hepatic lipase. Journal of Lipid Research, 43, 1352-1362.

[49] Doolittle, M. H., Ehrhardt, N., & Péterfy, M. (2010). Lipase maturation factor 1 (Lmf1): structure and role in lipase folding and assembly. Current Opinion in Lipidology, 21, 198-203.

[50] Brown, R. J., & Rader, D. J. (2007). Lipases as modulators of atherosclerosis in murine models. Current Drug Targets, 8, 1307-1319.

[51] Takahashi, M., Yagyu, H., Tazoe, F., Nagashima, S., Ohshiro, T., Okada, K., Osuga, J., Goldberg, I. J., & Ishibashi, S. (2013). Macrophage lipoprotein lipase modulates the development of atherosclerosis but not adiposity. Journal of Lipid Research, 54, 1124-1134.

[52] Wilson, K., Fry, G. L., Chappell, D. A., Sigmund, C. D., & Medh, J. D. (2001). Macrophage-specific expression of human lipoprotein lipase accelerates atherosclerosis in transgenic apolipoprotein e knockout mice but not in C57BL/6 mice. Arteriosclerosis, Thrombosis, and Vascular Biology, 21, 1809-1815.

[53] Den Hartigh, L. J., Connolly-Rohrbach, J. E., Fore, S., Huser, T. R., & Rutledge, J. C. (2010). Fatty acids from very low-density lipoprotein lipolysis products induce lipid droplet accumulation in human monocytes. The Journal of Immunology, 184, 3927-3936.

[54] Förstermann, U., Xia, N., & Li, H. (2017). Roles of vascular oxidative stress and nitric oxide in the pathogenesis of atherosclerosis. Circulation Research, 120, 713-735.

[55] Halliwell, B., & Gutteridge, J. M. (2015). Oxygen: Boon yet Bane-introducing oxygen toxicity and reactive species. Free Radicals in Biology and Medicine (5th ed.). Oxford university press, 1-29.

`

[56] Fukai, T., & Ushio-Fukai, M. (2011). Superoxide dismutases: role in redox signaling, vascular function, and diseases. Antioxidants & Redox Signaling, 15, 1583-1606.

[57] Haber, F., & Weiss, J. (1934). The catalytic decomposition of hydrogen peroxide by iron salts. Proceedings of the Royal Society of London. Series A-Mathematical and Physical Sciences, 147, 332-351.

[58] Arnhold, J. (2004). Properties, functions, and secretion of human myeloperoxidase. Biochemistry (Moscow), 69, 4-9.

[59] Corda, S., Laplace, C., Vicaut, E., & Duranteau, J. (2001). Rapid reactive oxygen species production by mitochondria in endothelial cells exposed to tumor necrosis factor-α is mediated by ceramide. American Journal of Respiratory Cell and Molecular Biology, 24, 762-768.

[60] Yang, D., Elner, S. G., Bian, Z. M., Till, G. O., Petty, H. R., & Elner, V. M. (2007). Pro-inflammatory cytokines increase reactive oxygen species through mitochondria and NADPH oxidase in cultured RPE cells. Experimental Eye Research, 85, 462-472.

[61] Grote, K., Flach, I., Luchtefeld, M., Akin, E., Holland, S. M., Drexler, H., & Schieffer, B. (2003). Mechanical stretch enhances mRNA expression and proenzyme release of matrix metalloproteinase-2 (MMP-2) via NAD(P)H oxidase–derived reactive oxygen species. Circulation Research, 92, e80-e86.

[62] Bedard, K., & Krause, K. H. (2007). The NOX family of ROS-generating NADPH oxidases: physiology and pathophysiology. Physiological Reviews, 87, 245-313.

[63] Gardiner, G. J., Deffit, S. N., McLetchie, S., Pérez, L., Walline, C. C., & Blum, J. S. (2013). A role for NADPH oxidase in antigen presentation. Frontiers in Immunology, 4, 295.

[64] Rueckschloss, U., Duerrschmidt, N., & Morawietz, H. (2003). NADPH oxidase in

`

endothelial cells: impact on atherosclerosis. Antioxidants and Redox Signaling, 5, 171-180.

[65] Bryk, D., Olejarz, W., & Zapolska-Downar, D. (2017). The role of oxidative stress and NADPH oxidase in the pathogenesis of atherosclerosis. Postepy Higieny i Medycyny Doswiadczalnej, 71, 57-68.

[66] Manea, S. A., Constantin, A., Manda, G., Sasson, S., & Manea, A. (2015). Regulation of Nox enzymes expression in vascular pathophysiology: focusing on transcription factors and epigenetic mechanisms. Redox Biology, 5, 358-366.

[67] Fulton, D. J., & Barman, S. A. (2016). Clarity on the isoform-specific roles of NADPH oxidases and NADPH oxidase-4 in atherosclerosis. Arteriosclerosis, Thrombosis, and Vascular Biology, 36, 579-581.

[68] Filomeni, G., De Zio, D., & Cecconi, F. (2015). Oxidative stress and autophagy: the clash between damage and metabolic needs. Cell Death & Differentiation, 22, 377-388.

[69] Schröder, K. (2014). NADPH oxidases in redox regulation of cell adhesion and migration. Antioxidants & Redox Signaling, 20, 2043-2058.

[70] Gray, S. P., Di Marco, E., Kennedy, K., Chew, P., Okabe, J., El-Osta, A., Jandeleit-Dahm, K. A.,Calkin, A. C., Biessen, E. A., Touyz, R. M., Cooper, M. E., & Schmidt, H. H. (2016). Reactive oxygen species can provide atheroprotection via NOX4- dependent inhibition of inflammation and vascular remodeling. Arteriosclerosis, Thrombosis, Vascular Biology, 36, 295-307.

[71] Gray, S. P., Di Marco, E., Okabe, J., Szyndralewiez, C., Heitz, F., Montezano, A. C., Jandeleit-Dahm, K. A., de Haan, J. B., Koulis, C., El-Osta, A., Andrews, K. L., Chin-Dusting, J. P., Touyz, R. M., Wingler, K., Cooper, M. E., & Schmidt, H. H.. (2013). NADPH oxidase 1 plays a key role in diabetes mellitus–accelerated atherosclerosis. Circulation, 127, 1888-1902.

`

[72] Schröder, K., Zhang, M., Benkhoff, S., Mieth, A., Pliquett, R., Kosowski, J., Kruse, C., Luedike, P., Michaelis, U. R., Weissmann, N., Dimmeler, S., Shah, A. M., & Brandes, R. P. (2012). Nox4 is a protective reactive oxygen species generating vascular NADPH oxidase. Circulation Research, 110, 1217-1225.

[73] Di Marco, E., Gray, S. P., Kennedy, K., Szyndralewiez, C., Lyle, A. N., Lassègue, B., Griendling, K. K., Cooper, M. E., Schmidt, H., & Jandeleit-Dahm, K.(2016). NOX4-derived reactive oxygen species limit fibrosis andinhibit proliferation of vascular smooth muscle cells in diabetic atherosclerosis. Free Radical Biology and Medicine, 97, 556-567.

[74] Schürmann, C., Rezende, F., Kruse, C., Yasar, Y., Löwe, O., Fork, C., van de Sluis, B., Bremer, R., Weissmann, N., Shah, A. M., Jo, H., Brandes, R. P., & Schröder, K.(2015). The NADPH oxidase Nox4 has anti-atherosclerotic functions. European Heart Journal, 36, 3447-3456.

[75] Guzik, T. J., Chen, W., Gongora, M. C., Guzik, B., Lob, H. E., Mangalat, D., Harrison, D. G.,Hoch, N., Dikalov, S. , Rudzinski, P., Kapelak, B., & Sadowskki, J. (2008). Calcium-dependent NOX5 nicotinamide adenine dinucleotide phosphate oxidase contributes to vascular oxidative stress in human coronary artery disease. Journal of theAmerican College of Cardiology, 52, 1803-1809.

[76] Liang, J., Wen, J., Huang, Z., Chen, X. P., Zhang, B. X., & Chu, L. (2019). Small nucleolar RNAs: insight into their function in cancer. Frontiers in Oncology, 9, 587.

[77] Esteller, M. (2011). Non-coding RNAs in human disease. Nature Reviews Genetics, 12, 861-874.

[78] Matera, A. G., Terns, R. M., & Terns, M. P. (2007). Non-coding RNAs: lessons from the small nuclear and small nucleolar RNAs. Nature Reviews Molecular Cell Biology, 8, 209-220.

`

[79] Reichow, S. L., Hamma, T., Ferré-D'Amaré, A. R., & Varani, G. (2007). The structure and function of small nucleolar ribonucleoproteins. Nucleic Acids Research, 35, 1452-1464.

[80] Brown, J. W., Marshall, D. F., & Echeverria, M. (2008). Intronic noncoding RNAs and splicing. Trends in Plant Science, 13, 335-342.

[81] Kiss-László, Z., Henry, Y., Bachellerie, J. P., Caizergues-Ferrer, M., & Kiss, T. (1996). Site-specific ribose methylation of preribosomal RNA: a novel function for small nucleolar RNAs. Cell, 85, 1077-1088.

[82] Tollervey, D., & Kiss, T. (1997). Function and synthesis of small nucleolar RNAs. Current Opinion in Cell Biology, 9, 337-342.

[83] Weinstein, L. B., & Steitz, J. A. (1999). Guided tours: from precursor snoRNA to functional snoRNP. Current Opinion in Cell Biology, 11, 378-384.

[84] Mattick, J. S., Makunin, I.V. (2006). Non-coding RNA. Human Molecular Genetics, 15, R17–R29.

[85] Decatur, W. A., & Fournier, M. J. (2002). rRNA modifications and ribosome function. Trends in Biochemical Sciences, 27, 344-351.

[86] Kehr, S., Bartschat, S., Tafer, H., Stadler, P. F., & Hertel, J. (2014). Matching of soulmates: coevolution of snoRNAs and their targets. Molecular Biology and Evolution, 31, 455-467.

[87] Bachellerie, J. P., Cavaillé, J., & Hüttenhofer, A. (2002). The expanding snoRNA world. Biochimie, 84, 775-790.

[88] Kiss-László, Z., Henry, Y., & Kiss, T. (1998). Sequence and structural elements of methylation guide snoRNAs essential for site-specific ribose methylation of pre-rRNA. The EMBO Journal, 17, 797-807.

`

[89] Darzacq, X., & Kiss, T. (2000). Processing of intron-encoded box C/D small nucleolar RNAs lacking a 5′, 3′-terminal stem structure. Molecular and Cellular Biology, 20, 4522-4531.

[90] Ganot, P., Caizergues-Ferrer, M., & Kiss, T. (1997). The family of box ACA small nucleolar RNAs is defined by an evolutionarily conserved secondary structure and ubiquitous sequence elements essential for RNA accumulation. Genes & Development, 11, 941-956.

[91] Kiss, T. (2001). Small nucleolar RNA-guided post-transcriptional modification of cellular RNAs. The EMBO Journal, 20, 3617-3622.

[92] Liang, X. H., Liu, Q., & Fournier, M. J. (2009). Loss of rRNA modifications in the decoding center of the ribosome impairs translation and strongly delays pre-rRNA processing. RNA 15, 1716-1728.

[93] Williams, G. T., Mourtada-Maarabouni, M., & Farzaneh, F. (2011). A critical role for non-coding RNA GAS5 in growth arrest and rapamycin inhibition in human T-lymphocytes. Biochemical Society Transactions, 39, 482-486.

[94] Thyagarajan, N., Marshall, J. D., Pickett, A. T., Schumacher, C., Yang, Y., Christian, S. L., & Brown, R. J. (2017). Transcriptomic analysis of THP-1 macrophages exposed to lipoprotein hydrolysis products generated by lipoprotein lipase. Lipids, 52, 189-205.

[95] Holley, C. L., Li, M. W., Scruggs, B. S., Matkovich, S. J., Ory, D. S., & Schaffer, J. E. (2015). Cytosolic accumulation of small nucleolar RNAs (snoRNAs) is dynamically regulated by NADPH oxidase. Journal of Biological Chemistry, 290, 11741-11748.

[96] Wang, L., Gill, R., Pedersen, T. L., Higgins, L. J., Newman, J. W., & Rutledge, J. C. (2009). Triglyceride-rich lipoprotein lipolysis releases neutral and oxidized FFAs that induce endothelial

`

cell inflammation. Journal of Lipid Research, 50, 204-213.

[97] Shen, X. Y., Gao, Z. K., Han, Y., Yuan, M., Guo, Y. S., & Bi, X. (2021). Activation and role of astrocytes in ischemic stroke. Frontiers in Cellular Neuroscience, 15, 755955.

[98] Duong, M. T., Nasrallah, I. M., Wolk, D. A., Chang, C. C., & Chang, T. Y. (2021). Cholesterol, atherosclerosis, and APOE in vascular contributions to cognitive impairment and dementia (VCID): potential mechanisms and therapy. Frontiers in Aging Neuroscience, 13, 142.

[99] Nomura, Y., Hirata, Y., Kiuchi, K., & Oh-Hashi, K. (2016). Translational and post-translational regulation of mouse cation transport regulator homolog 1. Scientific Reports, 6, 28016.

[100] Ku, H. C., & Cheng, C. F. (2020). Master regulator activating transcription factor 3 (ATF3) in metabolic homeostasis and cancer. Frontiers in Endocrinology, 11,556.

[101] Sebastián, V. P., Salazar, G. A., Coronado-Arrázola, I., Schultz, B. M., Vallejos, O. P., Berkowitz, L., Álvarez-Lobos, M. M., Riedel, C. A., Kalergis, A. M., & Bueno, S. M. (2018). Heme oxygenase-1 as a modulator of intestinal inflammation development and progression. Frontiers in Immunology, 9, 1956.

[102] Li, R. A., Traver, D., Matthes, T., & Bertrand, J. Y. (2016). Ndrg1b and fam49ab modulate the PTEN pathway to control T-cell lymphopoiesis in the zebrafish. Blood, The Journal of the American Society of Hematology, 128, 3052-3060.

[103] Wang, W., Cho, H. S., Kim, R., Jancarik, J., Yokota, H., Nguyen, H. H., Kim, S. H., Grigoriev, I. V., & Wemmer, D. E. (2002). Structural characterization of the reaction pathway in phosphoserine phosphatase: crystallographic “snapshots” of intermediate states. Journal of Molecular Biology, 319, 421-431.

`

[104] Keyse, S. M. (2008). Dual-specificity MAP kinase phosphatases (MKPs) and cancer. Cancer and Metastasis Reviews, 27, 253-261.

[105] Liu, Y., Wei, Z., Ma, X., Yang, X., Chen, Y., Sun, L., Ma, C., Miao, Q. R., Hajjar, D. P., Han, J., & Duan, Y. (2018). 25- Hydroxycholesterol activates the expression of cholesterol 25-hydroxylase in an LXR-dependentmechanism. Journal of Lipid Research, 59, 439-451.

[106] Tanaka, T., Narazaki, M., & Kishimoto, T. (2014). IL-6 in inflammation, immunity, and disease. Cold Spring Harbor Perspectives in Biology, 6, a016295.

[107] Schoggins, J. W., Wilson, S. J., Panis, M., Murphy, M. Y., Jones, C. T., Bieniasz, P., & Rice, C. M. (2011). A diverse range of gene products are effectors of the type I interferon antiviral response. Nature, 472, 481-485.

[108] Martinerie, L., Manterola, M., Chung, S. S., Panigrahi, S. K., Weisbach, M., Vasileva, A., Geng, Y., Sicinski, P., & Wolgemuth, D. J. (2014). Mammalian E-type cyclins control chromosome pairing, telomere stability and CDK2 localization in male meiosis. PLoS Genetics, 10, e1004165.

[109] Edagawa, M., Kawauchi, J., Hirata, M., Goshima, H., Inoue, M., Okamoto, T., Kitajima, S. Murakami, A., & Maehara, Y. (2014). Role of activating transcription factor 3 (ATF3) in endoplasmic reticulum (ER) stress-induced sensitization of p53-deficient human colon cancer cells to tumor necrosis factor (TNF)-related apoptosis-inducing ligand (TRAIL)-mediated apoptosis through up-regulation of death receptor 5 (DR5) by zerumbone and celecoxib. Journal of Biological Chemistry, 289,21544-21561.

[110] Gold, E. S., Ramsey, S. A., Sartain, M. J., Selinummi, J., Podolsky, I., Rodriguez, D. J., Moritz, R. L., & Aderem, A. (2012). ATF3 protects against atherosclerosis by suppressing 25-hydroxycholesterol–induced lipid body formation. Journal of Experimental Medicine, 209,

`

807-817.

[111] Lee-Rueckert, M., Lappalainen, J., Kovanen, P. T., & Escola-Gil, J. C. (2022). Lipid-laden macrophages and inflammation in atherosclerosis and cancer: an integrative view. Frontiers in Cardiovascular Medicine, 9,777822.

[112] Babaev, V. R., Patel, M. B., Semenkovich, C. F., Fazio, S., & Linton, M. F. (2000). Macrophage lipoprotein lipase promotes foam cell formation and atherosclerosis in low density lipoprotein receptor-deficient mice. Journal of Biological Chemistry, 275, 26293-26299.

[113] Babaev, V. R., Fazio, S., Gleaves, L. A., Carter, K. J., Semenkovich, C. F., & Linton, M. F. (1999). Macrophage lipoprotein lipase promotes foam cell formation and atherosclerosis in vivo. The Journal of Clinical Investigation, 103, 1697-1705.

[114] Leopold, J. A., & Loscalzo, J. (2008). Oxidative mechanisms and atherothrombotic cardiovascular disease. Drug Discovery Today: Therapeutic Strategies, 5, 5-13.

[115] Huber, A. H., & Kleinfeld, A. M. (2017). Unbound free fatty acid profiles in human plasma and the unexpected absence of unbound palmitoleate. Journal of Lipid Research, 58, 578-585.

[116] Schönfeld, P., & Wojtczak, L. (2008). Fatty acids as modulators of the cellular production of reactive oxygen species. Free Radical Biology and Medicine, 45, 231-241.

[117] Gonzalez, C., Agapito, M. T., Rocher, A., Gonzalez-Martin, M. C., Vega-Agapito, V., Gomez-Niño, A., Rigual, R., Castañeda, J., & Obeso, A. (2007). Chemoreception in the context of the general biology of ROS. Respiratory Physiology & Neurobiology, 157, 30-44.

[118] Shiose, A., & Sumimoto, H. (2000). Arachidonic acid and phosphorylation synergistically induce a conformational change of p47 phox to activate the phagocyte NADPH oxidase. Journal

`

of Biological Chemistry, 275, 13793-13801.

[119] Nigorikawa, K., Okamura, N., & Hazeki, O. (2004). The effect of anionic amphiphiles on the recruitment of Rac in neutrophils. Journal of Biochemistry, 136, 463-470.

[120] Taylor, R. M., Foubert, T. R., Burritt, J. B., Baniulis, D., McPhail, L. C., & Jesaitis, A. J. (2004). Anionic amphiphile and phospholipid-induced conformational changes in human neutrophil flavocytochrome b observed by fluorescence resonance energy transfer. Biochimica et Biophysica Acta - Biomembranes, 1663, 201-213.

[121] da Costa, R. M., Rodrigues, D., Pereira, C. A., Silva, J. F., Alves, J. V., Lobato, N. S., & Tostes, R. C. (2019). Nrf2 as a potential mediator of cardiovascular risk in metabolic diseases. Frontiers in Pharmacology, 10, 382.

[122] Tebay, L. E., Robertson, H., Durant, S. T., Vitale, S. R., Penning, T. M., Dinkova-Kostova, A. T., & Hayes, J. D. (2015). Mechanisms of activation of the transcription factor Nrf2 by redox stressors, nutrient cues, and energy status and the pathways through which it attenuates degenerative disease. Free Radical Biology and Medicine, 88, 108-146.

[123] Forman, H. J., & Torres, M. (2002). Reactive oxygen species and cell signaling: respiratory burst in macrophage signaling. American journal of Respiratory and Critical Caremedicine, 166, S4-S8.

[124] Zorov, D. B., Juhaszova, M., & Sollott, S. J. (2014). Mitochondrial reactive oxygen species (ROS) and ROS-induced ROS release. Physiological Reviews, 94, 909-950.

[125] Adam-Vizi, V., & Tretter, L. (2013). The role of mitochondrial dehydrogenases in the generation of oxidative stress. Neurochemistry International, 62, 757-763.

[126] Starkov, A. A., Fiskum, G., Chinopoulos, C., Lorenzo, B. J., Browne, S. E., Patel, M. S., &

`

Beal, M. F. (2004). Mitochondrial α-ketoglutarate dehydrogenase complex generates reactive oxygen species. Journal of Neuroscience, 24, 7779-7788.

[127] Di Meo, S., Reed, T. T., Venditti, P., & Victor, V. M. (2016). Role of ROS and RNS sources in physiological and pathological conditions. Oxidative Medicine and Cellular Longevity,2016, 1245049.

[128] Gao, Y., Moten, A., & Lin, H. K. (2014). Akt: a new activation mechanism. Cell Research, 24, 785-786.

[129] Arcaro, A., & Guerreiro, A. S. (2007). The phosphoinositide 3-kinase pathway in human cancer: genetic alterations and therapeutic implications. Current Genomics, 8, 271-306.

[130] Marshall, J. D., Courage, E. R., Elliott, R. F., Fitzpatrick, M. N., Kim, A. D., Lopez-Clavijo, A. F., Woolfrey, B. A., Ouimet, M., Wakelam, M., & Brown, R. J. (2020). THP-1 macrophage cholesterol efflux is impaired bypalmitoleate through Akt activation. PloS One, 15, e0233180.

[131] Nakanishi, A., Wada, Y., Kitagishi, Y., & Matsuda, S. (2014). Link between PI3K/AKT/PTEN pathway and NOX proteinin diseases. Aging and Disease, 5, 203.

[132] Zhao, Y., Qian, Y., Sun, Z., Shen, X., Cai, Y., Li, L., & Wang, Z. (2021). Role of PI3K in the Progression and Regression of Atherosclerosis. Frontiers in Pharmacology, 12, 263.

[133] Rensing, K. L., de Jager, S. C., Stroes, E. S., Vos, M., Twickler, M. T. B., Dallinga-Thie, G. M., von der Thüsen, J. H., de Vries, C. J., Kuiper, J., & Bot, I. (2014). Akt2/LDLr double knockout mice display impairedglucose tolerance and develop more complex atherosclerotic plaques than LDLr knockout mice. Cardiovascular Research, 101, 277-287.

[134] Babaev, V. R., Hebron, K. E., Wiese, C. B., Toth, C. L., Ding, L., Zhang, Y., May, J. M., Fazio, S., Vickers, K. C., & Linton, M. F. (2014). Macrophage deficiency of Akt2 reduces

`

atherosclerosis in Ldlr null mice [S]. Journal of Lipid Research, 55, 2296-2308.

[135] Rodlan, N., Chamorro-Jorganes, A., Araldi, E., Wanschel, A. C., Aryal, B., Aranda, J. F., Fernández-Hernando, C., Goedeke, L., Salerno, A. G.,Ramirez, C.M., Sessa, Y. S. & Suarez, Y.(2015). Hematopoietic Akt2 deficiency attenuates the progression of atherosclerosis. The FASEB Journal, 29, 597-610.

[136] Zhang, Y., Wang, X., Yang, H., Liu, H., Lu, Y., Han, L., & Liu, G. (2013). Kinase AKT controls innate immune cell development and function. Immunology, 140, 143-152.

[137] Amir, S., Hartvigsen, K., Gonen, A., Leibundgut, G., Que, X., Jensen-Jarolim, E., Wagner, O., Tsimikas, S., Witztum, J. L., & Binder, C. J. (2012). Peptide mimotopes of malondialdehyde epitopes for clinical applications in cardiovascular disease. Journal of Lipid Research, 53, 1316-1326.

[138] Yu, H., Littlewood, T., & Bennett, M. (2015). Akt isoforms in vascular disease. Vascular Pharmacology, 71, 57-64.

[139] Gough, D. R., & Cotter, T. G. (2011). Hydrogen peroxide: a Jekyll and Hyde signalling molecule. Cell Death & Disease, 2, e213-e213.

[140] Arnold, R. S., Shi, J., Murad, E., Whalen, A. M., Sun, C. Q., Polavarapu, R., Lambeth, J. D., Parthasarathy, S., & Petros, J. A. (2001). Hydrogen peroxide mediates the cell growth and transformation caused by themitogenic oxidase Nox1. Proceedings of the National Academy of Sciences of the United States of America, 98, 5550-5555.

[141] Guzik, T. J., & Harrison, D. G. (2006). Vascular NADPH oxidases as drug targets for novel antioxidant strategies. Drug Discovery Today, 11, 524-533.

[142] Su, L. J., Zhang, J. H., Gomez, H., Murugan, R., Hong, X., Xu, D., Jiang, F., & Peng,

`

Z. Y.(2019). Reactive oxygen species-induced lipid peroxidation in apoptosis, autophagy, and ferroptosis. Oxidative Medicine and Cellular Longevity, 2019, 1–13.

[143] Elkin, E. R., Harris, S. M., & Loch-Caruso, R. (2018). Trichloroethylene metabolite S-(1, 2-dichlorovinyl)-l-cysteine induces lipid peroxidation-associated apoptosis via the intrinsic and extrinsic apoptosis pathways in a first-trimester placental cell line. Toxicology and Applied Pharmacology, 338, 30-42.

[144] Chaudhary, P., Sharma, R., Sharma, A., Vatsyayan, R., Yadav, S., Singhal, S. S., Awasthi, Y. C, Rauniyar, N., & Prokai, L., Awasthi, S. (2010). Mechanisms of 4-hydroxy-2-nonenal induced pro-and anti-apoptoticsignaling. Biochemistry, 49, 6263-6275.

[145] Giacco, F., & Brownlee, M. (2010). Oxidative stress and diabetic complications. Circulation Research, 107, 1058-1070.

[146] Brooks, A. C., Guo, Y., Singh, M., McCracken, J., Xuan, Y. T., Srivastava, S., Bhatnagar, A. & Bolli, R., (2014). Endoplasmic reticulum stress-dependent activation of ATF3 mediates the latephase of ischemic preconditioning. Journal of Molecular and Cellular Cardiology, 76, 138-147.

[147] Gilchrist, M., Thorsson, V., Li, B., Rust, A. G., Korb, M., Roach, J. C., Kennedy, K., Hai, T., Bolouri, H., & Aderem, A. (2006). Systems biology approaches identify ATF3 as a negative regulator of Toll-like receptor 4. Nature, 441, 173-178.

[148] Kim, K. H., Jeong, J. Y., Surh, Y. J., & Kim, K. W. (2010). Expression of stress-response ATF3 is mediated by Nrf2 in astrocytes. Nucleic Acids Research, 38, 48-59.

[149] Tonelli, C., Chio, I. I. C., & Tuveson, D. A. (2018). Transcriptional regulation by Nrf2. Antioxidants & Redox Signaling, 29, 1727-1745.

`

[150] Ishikawa, K., Sugawara, D., Wang, X. P., Suzuki, K., Itabe, H., Maruyama, Y., & Lusis, A. J. (2001). Heme oxygenase-1 inhibits atherosclerotic lesion formation in LDL-receptor knockout mice. Circulation Research, 88, 506-512.

[151] Lee, T. S., Tsai, H. L., & Chau, L. Y. (2003). Induction of heme oxygenase-1 expression in murine macrophages is essential for the anti-inflammatory effect of low dose 15-deoxy-Δ12, 14-prostaglandin J2. Journal of Biological Chemistry, 278, 19325-19330.

[152] Philippidis, P., Mason, J. C., Evans, B. J., Nadra, I., Taylor, K. M., Haskard, D. O., & Landis, R. C. (2004). Hemoglobin scavenger receptor CD163 mediates interleukin-10 release and heme oxygenase-1 synthesis: antiinflammatory monocyte-macrophage responses in vitro, in resolving skin blisters in vivo, and after cardiopulmonary bypass surgery. Circulation Research, 94, 119-126.

[153] Orozco LD, Kapturczak MH, Barajas B, Wang X, Weinstein MM, Wong J, Deshane J, Bolisetty S, Shaposhnik Z, Shih DM, Agarwal A.(2007). Heme oxygenase-1 expression in macrophages plays a beneficial role in atherosclerosis. Circulation Research, 100, 1703-11.

[154] Levonen, A. L., Inkala, M., Heikura, T., Jauhiainen, S., Jyrkkänen, H. K., Kansanen, E., Määttä, K., Romppanen, E., Turunen, P., Rutanen, J., & Ylä-Herttuala, S. (2007). Nrf2 gene transfer induces antioxidant enzymes and suppresses smooth muscle cell growth in vitro and reduces oxidative stress in rabbit aorta in vivo. Arteriosclerosis, Thrombosis, and Vascular Biology, 27, 741-747.

[155] Swindell, W. R., Bojanowski, K., & Chaudhuri, R. K. (2020). A novel fumarate, isosorbide di-(methyl fumarate) (IDMF), replicates astrocyte transcriptome responses to dimethyl fumarate (DMF) but specifically down-regulates genes linked to a reactive phenotype. Biochemical and Biophysical Research Communications, 532, 475-481.

`

[156] Qin, J., Tao, D., Chen, X., Feng, Y., Hu, J., Reed, E., Li, Q. Q., & Gong, J. (2004). Down-regulation of cyclin E expression by caffeine promotes cancer cell entry into the S-phase of the cell cycle. Anticancer Research, 24, 2991-2996.

`